14

Intersubband and Interband Absorptions in Near-Surface Quantum Wells Under Intense Laser Field

Nicoleta Eseanu
Physics Department, "Politehnica" University of Bucharest, Bucharest
Romania

1. Introduction

The intersubband transitions in quantum wells have attracted much interest due to their unique characteristics: a large dipole moment, an ultra-fast relaxation time, and an outstanding tunability of the transition wavelengths (Asano et al., 1998; Elsaesser, 2006; Helm, 2000). These phenomena are not only important by the fundamental physics point of view, but novel technological applications are expected to be designed.

Many important devices based on intersubband transitions in quantum well heterostructures have been reported. For example: far- and near-infrared photodetectors (Alves et al., 2007; Levine, 1993; Li, S.S. 2002; Liu, 2000; Schneider & Liu, 2007; West & Eglash, 1985), ultrafast all-optical modulators (Ahn & Chuang, 1987; Carter et al., 2004; Li, Y. et al., 2007), all optical switches (Iizuka et al., 2006; Noda et al., 1990), and quantum cascade lasers (Belkin et al., 2008; Chakraborty & Apalkov, 2003; Faist et al., 1994).

It is well-known that the optical properties of the quantum wells mainly depend on the asymmetry of the confining potential experienced by the carriers. Such an asymmetry in potential profile can be obtained either by applying an electric/laser field to a symmetric quantum well (QW) or by compositionally grading the QW. In these structures the changes in the absorption coefficients were theoretically predicted and experimentally confirmed to be larger than those occurred in conventional square QW (Karabulut et al., 2007; Miller, D.A.B. et al., 1986; Ozturk, 2010; Ozturk & Sökmen, 2010).

In recent years, with the availability of intense THz laser sources, a large number of strongly laser-driven semiconductor heterostructures were investigated (Brandi et al., 2001; Diniz Neto & Qu, 2004; Duque, 2011; Eseanu et al., 2009; Eseanu, 2010; Kasapoglu & Sokmen, 2008; Lima, F. M. S. et al., 2009; Niculescu & Burileanu, 2010b; Ozturk et al., 2004; Ozturk et al., 2005; Sari et al., 2003; Xie, 2010).

These works have revealed important laser-induced effects:

i) the confinement potential is dramatically modified; ii) the energy levels of the electrons and, to a lesser extent, those of the holes are enhanced; iii) the linear and nonlinear absorption coefficients can be easily controlled by the confinement parameters in competition with the laser field intensity.

The intersubband transitions (ISBTs) have been observed in many different material systems. In recent years, apart from GaAs/AlGaAs, the InGaAs/GaAs QW structures have

attracted much interest because of their promising applications in optoelectronic and microelectronic devices: multiple-quantum-well modulators and switches (Stohr et al., 1993), broadband photodetectors (Gunapala et al., 1994; Li J. et al., 2010, Passmore, et al., 2007), superluminescent diodes used for optical coherence tomography (Li Z. et al., 2010) and metal-oxide-semiconductor field-effect-transistors, i. e. MOSFETs (Zhao et al., 2010). The optical absorption associated with the excitons in semiconductor QWs have been the subject of a considerable amount of work for the reason that the exciton binding energy and oscillator strength in QWs are considerably enhanced due to quantum confinement effect (Andreani & Pasquarello, 1990; Jho et al., 2010; Miller, R. C. et al., 1981; Turner et al., 2009; Zheng & Matsuura, 1998).

As a distinctive type of dielectric quantum wells, the near-surface quantum wells (n-sQWs) have involved increasing attention due to their potential to sustain electro-optic operations under a wide range of applied electric fields. In these heterostructures the QW is located close to vacuum and, as a consequence, the semiconductor-vacuum interface which is parallel to the well plane introduces a remarkable discrepancy in the dielectric constant (Chang & Peeters, 2000). This dielectric mismatch leads to a significant enhancement of the exciton binding energy (Gippius et al., 1998; Kulik et al., 1996; Niculescu & Eseanu, 2010a) and, consequently, it changes the exciton absorption spectra as some experimental (Gippius et al., 1998; Kulik et al., 1996; Li, Z. et al., 2010; Yablonskii et al., 1996) and theoretical (Niculescu & Eseanu, 2011a; Yu et al., 2004) studies have demonstrated.

The rapid advances in modern growth techniques and researches for InGaAs/GaAs QWs (Schowalter et al., 2006; Wu, S. et al., 2009) create the possibility to fabricate such heterostructures with well-controlled dimensions and compositions. Therefore, the differently shaped InGaAs/GaAs near-surface QWs become interesting and worth studying systems.

We expect that the capped layer of these n-sQWs induces considerable modifications on the intersubband absorption as it did on the interband excitonic transitions (Niculescu & Eseanu, 2011). To the best of our knowledge this is the first research concerning the intense laser field effect on the ISBTs in InGaAs/GaAs differently shaped near-surface QWs.

In this chapter we are concerned about the intersubband and interband optical transitions in differently shaped n-sQWs with symmetrical/asymmetrical barriers subjected to intense high-frequency laser fields. We took into account an accurate form for the laser-dressing confinement potential as well as the occurrence of the image-charges. Within the framework of a simple two-band model the consequences of the laser field intensity and carriers-surface interaction on the absorption spectra have been investigated.

The organization of this work is as follows. In Section 2 the theoretical model for the intense laser field (ILF) effect on the intersubband absorption in differently shaped n-sQWs is described together with numerical results for the electronic energy levels and absorption coefficients (linear and nonlinear). In Section 3 we explain the ILF effect on the exciton ground energy and interband transitions in the same QWs, taking into account the repulsive interaction between carriers and their image-charges. Also, numerical results for the 1S-exciton binding energy and interband linear absorption coefficient are discussed. Finally, our conclusions are summarized in Section 4.

2. Intersubband transitions in near-surface QWs under intense laser field

The intersubband transitions (ISBTs) are optical transitions between quasi-two-dimensional electronic states ("subbands") in semiconductors which are formed due to the confinement

of the electron wave function in one dimension. The conceptually simplest band-structure engineered system that can be fabricated is a quantum well (QW), which consists of a thin semiconductor layer embedded in another semiconductor with a larger bandgap. Depending on the relative band offsets of the two semiconductor materials, both electrons and holes can be confined in one direction in the conduction band (CB) and the valence band (VB), respectively. Thus, allowed energy levels which are quantized along the growth direction of the heterostructure appear (Yang, 1995). These levels can be tailored by changing the QW geometry (shape, width, barrier heights) or by applying external perturbations (hydrostatic pressure, electric, magnetic and laser fields). Whereas, of course, optical transitions can take place between VB and CB states, in this Section we are concerning only with ISBTs between quantized levels within the CB.

2.1 Theory

Let us consider an InGaAs n-sQW embedded between symmetrical/asymmetrical GaAs barriers. It is convention to define the QW growth as the z-axis. According to the effective mass approximation, in the absence of the laser field, the time-independent Schrödinger equation is

$$-\frac{\hbar^2}{2m^*}\frac{\partial^2}{\partial z^2}\varphi(z)+\left[V(z)+V_{self}(z)\right]\varphi(z)=E\varphi(z)\,. \tag{1}$$

where m^* is the electron effective mass, $V(z)$ is the confinement potential in the QW growth direction and $V_{self}(z)$ describes the repulsive interaction in the system consisting of an electron and its image-charge.

$$V_{self}(z)=\frac{e_0^2}{2\varepsilon}\left(\frac{\varepsilon-1}{\varepsilon+1}\right)\frac{1}{2d_0}\,. \tag{2}$$

Here ε is the semiconductor dielectric constant, $e_0^2=e^2/4\pi$, and d_0 is the distance between the electron and its image-charge without laser field. For the three differently shaped n-sQWs studied in this work the potential $V(z)$ reads as follows. For a square n-sQW, $V(z)$ has the well-known form

$$V^{SQW}(z)=\begin{cases}\infty, & z<-L_c\\ V_0, & -L_c<z<0 \;and\; z>L_w\\ 0, & 0\le z\le L_w\end{cases}\quad` \tag{3a}$$

For a graded n-sQW, the confinement potential is

$$V^{GQW}(z)=\begin{cases}\infty, & z<-L_c\\ V_0, & -L_c<z<0\\ V_r\dfrac{z}{2L_w}, & 0\le z\le L_w\\ V_r=\sigma V_0, & z>L_w\end{cases} \tag{3b}$$

For a semiparabolic n-sQW, $V(z)$ is given by

$$V^{sPQW}(z)=\begin{cases}\infty, & z<-L_c\\ V_0, & -L_c<z<0\\ V_r\left(\dfrac{z}{L_w}\right)^2, & 0\le z\le L_w\\ V_r=\sigma V_0, & z>L_w\end{cases} \tag{3c}$$

The quantities L_w and L_c are the well width and capped layer thicknesses, respectively; V_0 is the GaAs barrier height in the QW left side (with cap layer); V_r is the barrier height in the QW right side and σ is the barrier asymmetry parameter.

Under the action of a non-resonant intense laser field (ILF) represented by a monochromatic plane wave of frequency ω_{LF} having the vector potential $\vec{A}(t)=\vec{u}A_0\cos(\omega_{LF}t)$, the Schrödinger equation to be solved becomes a time-dependent one due to the time-dependent nature of the radiation field. Here $\vec{u}$ is the unit vector of the polarization direction (chosen as *z*-axis). By applying the translation $\vec{r}\to\vec{r}+\vec{\alpha}(t)$ the equation describing the electron-field interaction dynamics was transformed by Kramers (Kramers, 1956) as

$$-\frac{\hbar^2}{2m^*}\Delta\Psi(\vec{r},t)+V\left(\vec{r}+\vec{\alpha}(t)\right)\Psi(\vec{r},t)=i\hbar\frac{\partial}{\partial t}\Psi(\vec{r},t). \tag{4}$$

The expression

$$\vec{\alpha}(t)=\vec{u}\alpha_0\sin(\omega_{LF}t) \tag{5}$$

describes the quiver motion of the electron under laser field action. α_0 is known as the laser-dressing parameter, i. e. a laser-dependent quantity which contains both the laser frequency and intensity,

$$\alpha_0=\frac{eA_0}{m^*\omega_{LF}}. \tag{6}$$

Thus, in the presence of the laser field linearly polarized along the *z*-axis, the confinement potential $V\left(z+\alpha(t)\right)$ is a time-periodic function for a given *z* and it can be expanded in a Fourier series,

$$V\left(z+\alpha(t)\right)=\sum_k\sum_{v=-\infty}^{\infty}(-1)^v V_k J_v(k\alpha_0)\exp(ikz)\exp(-iv\omega_{LF}t) \tag{7}$$

where V_k is the *k*-th Fourier component of $V(z)$ and J_v is the Bessel function of order *v*. In the high-frequency limit, i.e. $\omega_{LF}\tau>>1$, with τ being the transit time of the electron in the QW region (Marinescu & Gavrila, 1995) the electron "sees" a laser-dressed potential which is obtained by averaging the potential $V\left(z+\alpha(t)\right)$ over a laser field period,

$$\tilde{V}(z,\alpha_0)=\frac{\omega_{LF}}{2\pi}\int_0^{2\pi/\omega_{LF}} V\left(z+\alpha(t)\right)dt=\sum_k V_k J_0(k\alpha_0)\exp(ikz). \tag{8}$$

Note that this approximation remains valid provided that the laser is tuned far from any resonance so that only photon absorption was taken into account and photon emission was disregarded.

Following some basic works (Gavrila & Kaminski, 1984; Lima, C.A.S. & Miranda, 1981; Marinescu & Gavrila, 1995) the laser-dressed electronic eigenstates in the QW are the solutions of a time-independent Schrödinger equation,

$$\left[-\frac{\hbar^2}{2}\frac{d}{dz}\left(\frac{1}{m^*(z)}\frac{d}{dz}\right)+\tilde{V}(z,\alpha_0)\right]\tilde{\varphi}(z)=E\,\tilde{\varphi}(z). \tag{9}$$

Here $\tilde{\varphi}(z)$ is the laser-dressed wave function of the electron. The envelope wave functions and subband energies in this modified potential can be obtained by using a transfer matrix method (Ando & Ytoh, 1987; Tsu & Esaki, 1973).

In order to characterize the intersubband transitions in laser-dressed n-sQWs the $E_1\to E_2$ transition energy, $E_{tr}=E_2-E_1$, and square of the optical matrix element, M_{21}^2, are worth being calculated. Our results for n-sQWs revealed that these quantities depend on the QW width and shape as well as on laser field parameter and cap layer thickness.

The dipole matrix element of the $E_i\to E_f$ transition is defined by

$$M_{fi}=\int\varphi_f^*|e|z\varphi_i dz \tag{10}$$

Also, the first-order absorption coefficient, $\beta^{(1)}(\omega_{ex})$, and the third-order absorption coefficient, $\beta^{(3)}(\omega_{ex},I)$, for an optical transition between two subbands can be calculated by using the compact density matrix method (Bedoya & Camacho, 2005; Rosencher & Bois, 1991) and a typical iterative procedure (Ahn & Chuang, 1987). The linear and nonlinear absorption coefficients are written (Unlu et al., 2006; Ozturk, 2010) as:

$$\begin{aligned}\beta^{(1)}(\omega_{ex})&=\sqrt{\frac{\mu}{\varepsilon}}|M_{21}|^2\frac{m^*k_BT}{L_{eff}\pi\hbar^2}\\&\times\ln\left\{\frac{1+\exp\left[(E_F-E_1)/k_BT\right]}{1+\exp\left[(E_F-E_2)/k_BT\right]}\right\}\times\frac{\omega_{ex}\hbar/\tau_{in}}{(E_2-E_1-\hbar\omega_{ex})^2+(\hbar/\tau_{in})^2}\end{aligned} \tag{11}$$

$$\begin{aligned}\beta^{(3)}(\omega_{ex},I)&=-\sqrt{\frac{\mu}{\varepsilon}}\left(\frac{I}{2\varepsilon_0 n_r c}\right)|M_{21}|^2\frac{m^*k_BT}{L_{eff}\pi\hbar^2}\\&\times\ln\left\{\frac{1+\exp\left[(E_F-E_1)/k_BT\right]}{1+\exp\left[(E_F-E_2)/k_BT\right]}\right\}\times\frac{\omega_{ex}\hbar/\tau_{in}}{\left[(E_2-E_1-\hbar\omega_{ex})^2+(\hbar/\tau_{in})^2\right]^2}\end{aligned}$$

$$\times\left\{\begin{array}{l} 4\left|M_{21}\right|^2-\dfrac{\left|M_{22}-M_{11}\right|^2}{\left(E_2-E_1\right)^2+\left(\hbar/\tau_{in}\right)^2} \\ \times\left[\left(E_2-E_1-\hbar\omega_{ex}\right)^2-\left(\hbar/\tau_{in}\right)^2+2\left(E_2-E_1\right)\left(E_2-E_1-\hbar\omega_{ex}\right)\right] \end{array}\right\} \tag{12}$$

Here I is the optical intensity of the incident electromagnetic wave (with the angular frequency ω_{ex}) that excites the semiconductor nanostructure and leads to the intersubband optical transition, μ is the permeability, $\varepsilon=\varepsilon_0 n_r^2$ with n_r being the refractive index, $\hbar\omega_{ex}$ is the pump photon energy produced by a tunable laser source, E_F represents the Fermi energy, E_1 and E_2 denote the quantized energy levels for the initial and final states, respectively; k_B and T are the Boltzmann constant and temperature, respectively, c is the speed of light in free space, L_{eff} is the effective spatial extent of the electrons and τ_{in} is the intersubband relaxation time.
The total absorption coefficient is given by

$$\beta\left(\omega_{ex},I\right)=\beta^{(1)}\left(\omega_{ex}\right)+\beta^{(3)}\left(\omega_{ex},I\right) \tag{13}$$

The absorbtion coefficients in n-sQWs under laser field depend on both laser-dressing parameter and QW geometry (well shape, barrier asymmetry, cap layer thickness).

2.2 Electronic properties

2.2.1 Laser-dressed confinement potential and energy levels

Within the framework of effective-mass approximation the ground and the first excited energetic levels for an electron confined in differently shaped $In_{0.18}Ga_{0.82}As/GaAs$ near-surface QWs: square (SQW), graded (GQW), and semiparabolic (sPQW) under high-frequency laser field were calculated. We used various QW widths L = 100 Å, 150 Å, and 200 Å, different cap layer thicknesses, L_c, between 5 Å and 200 Å, for n-sQWs with symmetrical (σ = 1) or asymmetrical (σ = 0.6 and 0.8) barriers. The small In atoms concentration in the QW layer allowed us to take the same value of the electron effective mass in all regions (barriers, QW), i. e. $m^*=0.0665\,m_0$. Also, we used E_F = 6.49 meV which corresponds to about 1.6 × 10^{17} electrons/cm^3 in GaAs, and τ_{in} = 0.14 ps (Ahn & Chuang, 1987).
Fig. 1 displays the "dressed" potential profiles of the conduction band (CB) for three differently shaped n-sQWs (SQW, GQW and sPQW) with QW width L_w = 150 Å, identical barriers (σ = 1) and cap layer thickness L_c = 20 Å, under various laser intensities described by the laser parameter values α_0 = 0; 40; 80 and 100 Å. Only two energy levels have been taken into account for all the n-sQWs investigated in this work: E_1 (ground state) and E_2 (first excited state). They are are plotted in Fig. 1, too.
We see that for all studied n-sQWs the increasing of the laser parameter dramatically modifies the potential shape which is responsible for quantum confinement of the electrons. Up to $\alpha_0 \le L_w/2$ two effects are noticeable: i) while the effective "dressed" well width (i. e. the lower part of the confinement potential) decreases with the laser intensity, the width of the upper part of this "dressed" QW increases; ii) a reduction of the effective well height at the interface between the capped layer and the QW (z = 0).

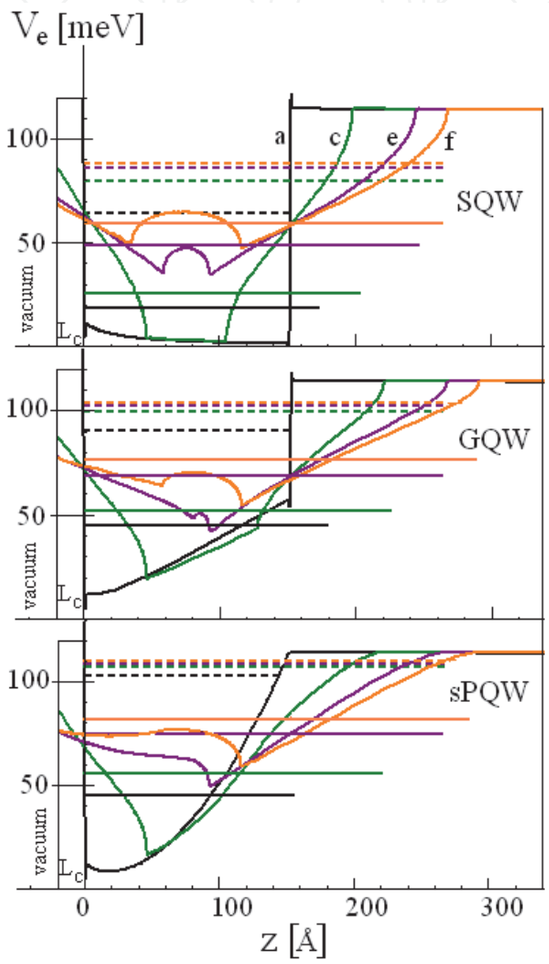

Fig. 1. (Color online) Laser-dressed confinement potentials of three differently shaped $In_{0.18}Ga_{0.82}As/GaAs$ near-surface QWs with identical barriers and the corresponding energy levels: ground state E_1 (solid lines) and first excited state E_2 (dashed lines). Notations a, c, e, and f stand for various laser parameter values, α_0 = 0 (black), 40 Å (olive), 80 Å (purple), and 100 Å (orange), respectively. QW width and cap layer thickness are L_w = 150 Å and L_c = 20 Å, respectively.

Therefore, under an intense laser field a distinctive blue-shift of the electronic energy levels occurs, as expected (Brandi et al., 2001; Diniz Neto & Qu, 2004; Eseanu, 2010; Kasapoglu & Sökmen, 2008; Lima, F. M. S. et al., 2009; Niculescu & Burileanu, 2010b; Ozturk et al., 2004; Ozturk et al., 2005). This laser-induced push-up effect is more pronounced in the semiparabolic QW due to the stronger geometric confinement.

For $\alpha_0 > L_w/2$ a supplementary barrier having a "hill"-form appears into the well region and, as a consequence, the formation of a double well potential in the InGaAs layer is predicted. Similar laser-induced phenomena were reported for a GaAs/AlGaAs square QW (Lima, F. M. S. et al., 2009) and for coaxial quantum wires (Niculescu & Radu, 2010c).

The two energy levels E_1 (ground state) and E_2 (first excited state) depend on both laser field characteristics (frequency and intensity, combined in the laser parameter) and QW confining geometry (shape, width, cap layer thickness and barrier asymmetry).

In Figs. 2 A-C the energy levels E_1 and E_2 are plotted as functions of laser parameter in three differently shaped n-sQWs (SQW, GQW and sPQW) with L_w = 200 Å for various cap layer thicknesses.

We observed that:

i. the laser-induced increasing of the ground level energy E_1 is more pronounced for $\alpha_0 >$ 40 Å in all three differently shaped n-sQWs with the same L_w ;

ii. the first excited level energy E_2 is almost unaltered by the laser field in the GQW and sPQW for $\alpha_0 >$ 40 Å; instead, in the SQW, E_2 has a significant rising.

The reasons are as follows: i) the ground level E_1 is localized in the lower part of the laser-dressed QW and it is significantly moved up only by an intense laser field; ii) in the GQW and sPQW the stronger geometric confinement competes with the laser-induced push-up of the energy levels. As a consequence, the excited level which is localized in the upper part becomes less sensitive to the laser action.

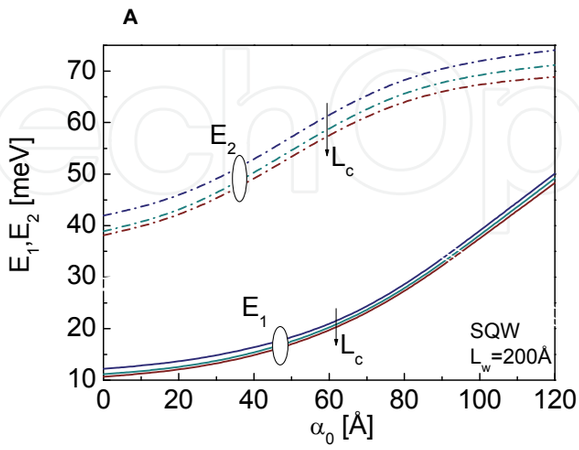

Fig. 2. A

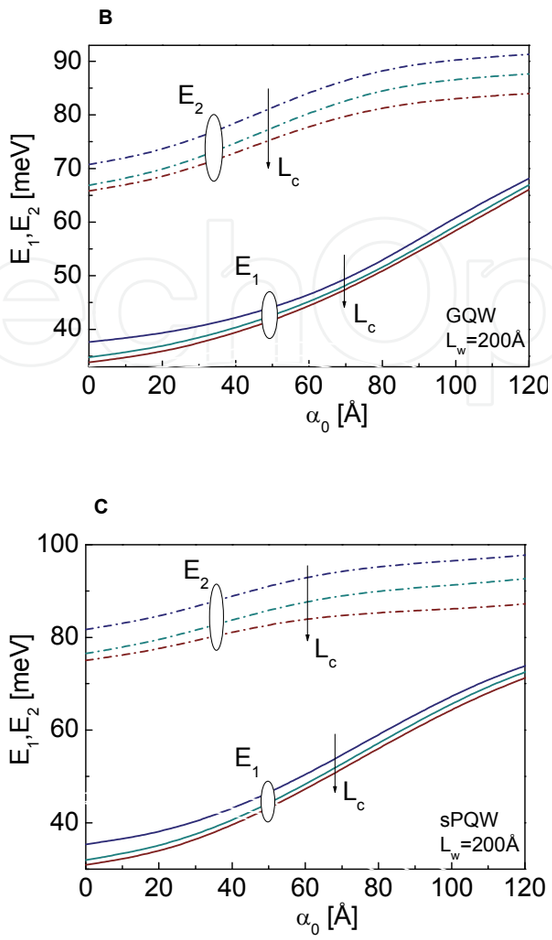

Fig. 2. Energy levels (ground state and first excited state) vs. laser parameter in three differently shaped n-sQWs: a) SQW, b) GQW and c) sPQW with L_w = 200 Å. Each arrow indicates the rising of the cap layer thickness.

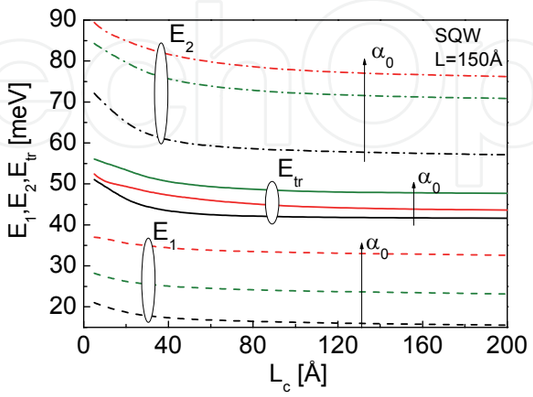

Fig. 3. Energy levels and transition energy vs. cap layer thickness in a near-surface SQW with L_w = 150 Å under various laser intensities. Each arrow indicates the rising of the laser parameter.

Also, in the range of thin cap layers, the energy levels E_1 and E_2 depend on the capped layer thickness (L_c). Fig. 3 displays the energies E_1, E_2 and transition energy, $E_{tr} = E_2 - E_1$, vs. L_c in a near-surface SQW with L_w = 150 Å for several values of the laser parameter. This variation is similar in GQW and sPQW.

We note that, up to $L_c \cong 40$ Å, the energies E_1, E_2 and, consequently, the transition energy first rapidly decrease with cap layer thickness and, for further large L_c values, these three quantities turn out to be insensitive to the dielectric effect afforded by the cap layer. The reason for this behavior is that the effect of the image-charge is reduced by a thicker cap layer.

2.2.2 The $E_1 \to E_2$ transition energy

As the intense laser field induces obvious changes in the electronic levels a noticeable dependence of the $E_1 \to E_2$ transition energy, $E_{tr} = E_2 - E_1$, on the laser parameter, α_0, is expected. Also, this energy is modified by the QW confining properties. Figs. 4 A-C present the grouped data plot of the E_{tr} and square of the dipole matrix element (in units of e^2), M_{21}^2, as functions of the laser parameter, for differently shaped n-sQWs with various cap layer, L_c = 20, 50, 100, 200 Å and the same width, L_w = 150 Å. For SQW and GQW (Figs. 4 A, B) the transition energy, E_{tr}, increases up to a certain value of the laser parameter, α_{0M}, and then it begin to decrease. The critical laser parameter, α_{0M}, increases for larger QWs (Table 1). A similar behavior have been reported for regular (i.e. uncapped) GaAs/AlGaAs SQW and PQW (Eseanu, 2010; Ozturk et al., 2004). As suggested by Ozturk et al. (2004), for $\alpha_0 < \alpha_{0M}$ the transition energy E_{tr} increases due to reduction of the effective "dressed" well width. Instead, for $\alpha_0 > \alpha_{0M}$ the subbands levels E_1 and E_2 tends to localize in the upper part of the laser-dressed well (which has a larger width) and thus they become closer to each other. Our calculations show a difference between the increasing rates of E_1 and E_2 values in SQW and GQW under laser field action. Therefore, E_{tr} may have a maximum for a certain value α_{0M}. This critical value of the laser parameter seems to have a weak dependence on the cap layer thickness (Table 1).

L [Å]	α_{0M} [Å] (L_c = 20 Å)	α_{0M} [Å] (L_c = 50 Å)	α_{0M} [Å] (L_c = 100 Å)	α_{0m} [Å] (L_c = 20 Å)	α_{0m} [Å] (L_c = 50 Å)	α_{0m} [Å] (L_c = 100 Å)
SQW;150	39.7	40.4	40.0	45.0	46.3	42.4
SQW;200	67.0	68.3	66.6	71.0	72.0	69.7
GQW;150	32.5	32.0	31.3	41.0	38.9	-
GQW;200	61.9	59.6	56.8	62.0	-	-

Table 1. Laser parameter critical values α_{0M} (for the maximum of E_{tr}) and α_{0m} (for the minimum of M_{21}^2).

For sPQW we note a different behavior, i.e. E_{tr} reduces monotonically as the laser parameter increases (Fig. 4C). The supplementary quantum confinement of the electron localization in sPQW comparing with SQW and GQW could be the explanation.

For the three studied QW structures and for all the widths under our investigation the values of E_{tr} are diminuted by increasing L_c (vertical arrows indicate the L_c rising). This

effect can be explained by the stronger reduction of the ground level energy values E_2 for larger L_c (Fig. 3).

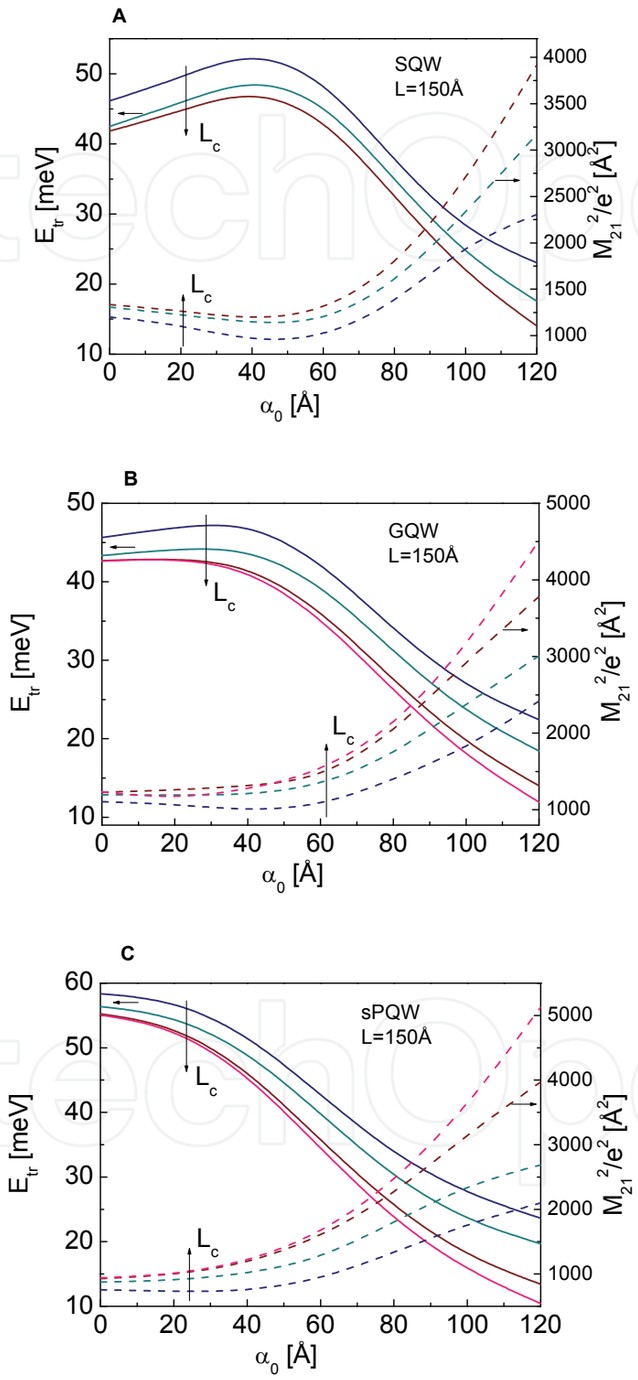

Fig. 4. Grouped data plot of the $E_1 \to E_2$ transition energy and the square of the matrix element (in units of e^2) vs. laser parameter, for differently shaped n-sQWs: A) square, B) graded, and C) semiparabolic, with various L_c.

Also, the transition energy depends on the QW width as Fig. 5 shows for a near-surface SQW with two values of the cap layer thickness, under several laser intensities.

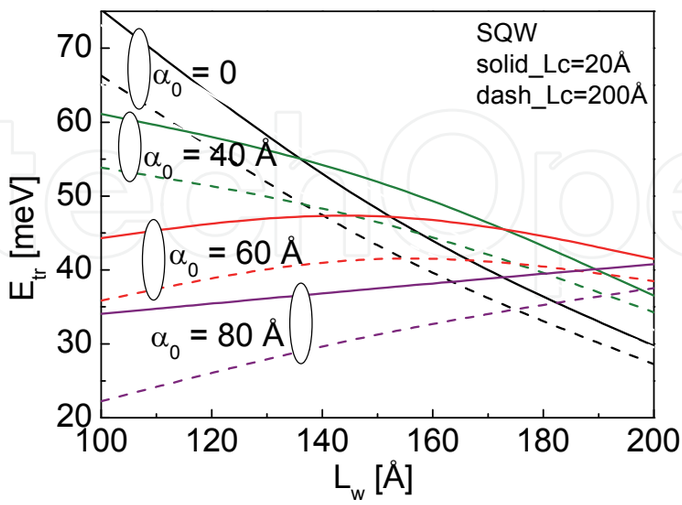

Fig. 5. Transition energy vs. QW width in a near-surface SQW for several laser parameters and two values of the cap layer thickness.

The variation of $E_{tr} = f(L_w)$ is modulated by the laser field. In the absence of radiation ($\alpha_0 = 0$) or in a low laser field ($\alpha_0 <$ 40 Å) E_{tr} diminishes in large QWs, as expected, because the levels E_1 and E_2 move down and become closer to each other. For uncapped QW-heterostructures this result is a customary one, for example: in a GaAs/$Al_{0.3}Ga_{0.7}$As SQW with L_w = 50 - 65 Å (Helm, 2000), in GaAs/$Al_{0.3}Ga_{0.7}$As SQW and sPQW with L_w = 100 - 200 Å (Eseanu, 2010) and in a $In_{0.5}Ga_{0.5}$As/AlAs SQW with L_w = 20 - 100 Å (Chui, 1994).

By applying an intense laser field the reduction of E_{tr} (as function of L_w) becomes weaker, but for high laser parameter values (α_0 = 80 Å), E_{tr} turn to rise with L_w, especially in the presence of a thick cap layer. The reason for this behavior is the competition between the geometric quantum confinement and laser-induced increasing of the energy levels.

In the asymmetrical n-sQWs (GQW and sPQW) another factor modifiying the transition energy appears. This is the asymmetry parameter of the QW barriers, σ, (see Eqs. 2b and 2c). In Fig. 6 the transition energy, E_{tr}, as a function of the barrier asymmetry is plotted for GQW and sPQW with L_w = 200 Å and a thin cap layer (20 Å). As seen in this figure E_{tr} is enhanced by the increasing σ. The dependence $E_{tr} = f(\sigma)$ is also modulated by the laser field and, to a lesser extent, by the QW shape.

In the GQW the increasing of E_{tr} is almost linear for all laser parameter values, but the rising slope is higher under intense laser field (α_0 = 80 Å) due to the laser-induced push-up effect on the energy levels. Instead, the stronger geometric confinement leads to a deviation from linearity of the curve $E_{tr} = f(\sigma)$ in the sPQW.

Now we should emphasize an important issue. As a consequence of the laser-induced shift in the subband transition energy it clearly appears the possibility that E_{tr} can be tuned by the joint action of the laser field and a supplementary external perturbation such as: electric

field (Ozturk et al., 2004; Ozturk et al., 2005) or hydrostatic pressure (Eseanu, 2010), these two cases refering to uncapped QWs. The last case was named "laser- and pressure-driven optical absorption" (LPDOA). The variable cap layer thickness, especially in the range of thin films, in simultaneous action with an intense laser field could be a new method (suggested by the present study) to adjust the transition energy, E_{tr} .

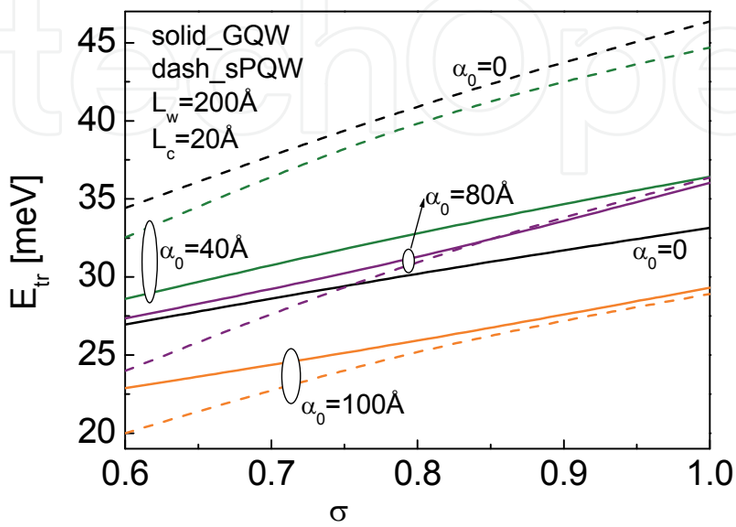

Fig. 6. Transition energy vs. asymmetry parameter of the QW barriers in GQW (solid lines) and sPQW (dashed lines) with L_w = 200 Å and L_c = 20 Å under various laser intensities.

2.2.3 The square dipole matrix element

The intense laser field strongly modifies the dipole matrix element of the $E_1 \to E_2$ transition, M_{21}^2, for all the three n-sQWs presented in this work, but in a different manner (Figs. 4 A, B, C).

In the symmetrical structure SQW (Fig. 4 A) M_{21}^2 has a relative minimum at a critical value α_{0m} of the laser parameter. This value is very close to that for which the transition energy E_{tr} has its maximum. A similar behavior have been reported for regular (i.e. uncapped) GaAs/AlGaAs SQWs (Eseanu, 2010). The explanation for the minimum of M_{21}^2 can be connected with the laser intensity dependent overlap of the two wave functions $\Psi_1(z)$ and $\Psi_2(z)$.

In the presence of laser field, the SQW shape is dramatically modified: as α_0 increases the lower part of the confinement potential becomes more and more narrow while the upper part becomes wider. Therefore, the energy subbands will be pushed up to the top of the well. We may identify two regimes:

i. for $\alpha_0 < \alpha_{0m}$ the second subband E_2 is localized in the upper part of the "dressed" well and the ground state E_1 is still localized in the lower part. As α_0 increases, the ground state wave function $\Psi_1(z)$ becomes more compressed in the vicinity of z = 0 and its overlap with the first excited wave function $\Psi_2(z)$ (which has a minimum in z = 0) reduces.

ii. by further increasing α_0, for $\alpha_0 > \alpha_{0m}$, the E_1 level is also pushed up to the wider upper part of the QW. Thus the carrier confinement decreases and the two wave functions $\Psi_1(z)$ and $\Psi_2(z)$ are spread out (or delocalized) in the potential barrier regions. As a consequence their overlapping is enhanced.

In the asymmetrical structures GQW and sPQW, M_{21}^2 monotonically increases with laser parameter (Figs. 4 B, C). This effect is determined by the strong electron localization in the graded barriers. Therefore, the two wave functions $\Psi_1(z)$, $\Psi_2(z)$ are localized in the upper part of the laser-dressed QW.

For the three studied n-sQWs and for all the widths under our investigation the values of M_{21}^2 are enhanced by growing L_c (vertical arrows indicate the L_c rising in Figs. 4 A, B, C). This effect can be explained by the broadening of the effective n-sQW width for thicker cap layers. Thus, the ground state wave function $\Psi_1(z)$ becomes more extended in the heterostructure and its overlap with the first excited wave function $\Psi_2(z)$ is enhanced.

2.3 Linear and nonlinear optical absorption

The intersubband linear and nonlinear absorption coefficients given by the Eqs. (11)-(12) depend on the transition energy, $E_{tr} = E_2 - E_1$, and on square of the dipole matrix element, M_{21}^2. In the n-sQWs under our investigation these quantities are strongly modified by the laser field parameter, but in a different manner (Fig. 4). As a consequence, the absorption coefficients $\beta^{(1)}(\omega_{ex})$ and $\beta^{(3)}(\omega_{ex}, I)$ are significantly changed by the laser intensity (included in the laser-dressing parameter α_0). However, there are still four variables to take into account: the pump photon energy, $\hbar\omega_{ex}$, cap layer thickness, L_c, asymmetry parameter of the QW barriers, σ, and QW potential shape.

In Fig. 7 the dependence of the linear absorption coefficient $\beta^{(1)}$ on the pump photon energy in differently shaped n-sQWs with L_w = 150 Å and symmetrical barriers, under various laser intensities α_0 = 0, 40 Å, and 80 Å, is plotted. The values of L_c are 20 Å and 200 Å

Fig. 8 displays the variation of $\beta^{(1)}$ on the pump photon energy in a near-surface SQW with L_c = 50 Å under various laser intensities α_0 = 0, 40 Å, and 80 Å. The values of L_w are 100 Å and 200 Å.

One can see from Figs. 7 and 8 that the increasing laser intensity generates a noticeable shift of the absorption peak position toward higher/lower photon energies and an obvious reduction of the $\beta^{(1)}$ magnitude. The trend of this shift significantly depends on the QW shape and width, also on the laser parameter. Several regimes occur:

1. in SQW and GQW with L_w = 150 Å the absorption peaks are blue-shifted for $\alpha_0 < L_w / 2$, but red-shifted for $\alpha_0 > L_w / 2$;
2. in GQW with L_w = 200 Å the absorption peaks (not plotted here) are blue-shifted for all the studied α_0 values, but the shift induced by a strong laser field (α_0 = 80 Å) is smaller;
3. in sPQW with L_w = 150 Å the linear absorption peaks are red-shifted for all the studied values of the laser parameter; a similar variation (not plotted here) was observed for L_w = 200 Å.
4. in SQW the absorption peaks are red-shifted for L_w = 100 Å, but for L_w = 200 Å they are blue-shifted (Fig. 8).

For SQW and GQW these effects can be connected with the different laser-dependence of the two energy levels E_1 and E_2 (Fig. 2). For sPQW the stronger geometric confinement competes with the laser-induced change of the transition energy. The explanation used for the results plotted in Fig. 4 remains valid for the absorption peak positions too. In all n-sQWs under our study the peak magnitude of the $\beta^{(1)}$ is diminuted by the laser field. The reason for this reduction is the laser-induced spreading of the carriers wave functions in the laser-dressed QW barriers.

Concerning the effect of the cap layer on the absorption peak position an obvious red-shift occurs for thicker cap layers, especially in sPQW (Fig. 7). The broadening of the effective n-sQW width for large cap layer thickness leading to a reduction of E_{tr} is the reason for this "dielectric effect".

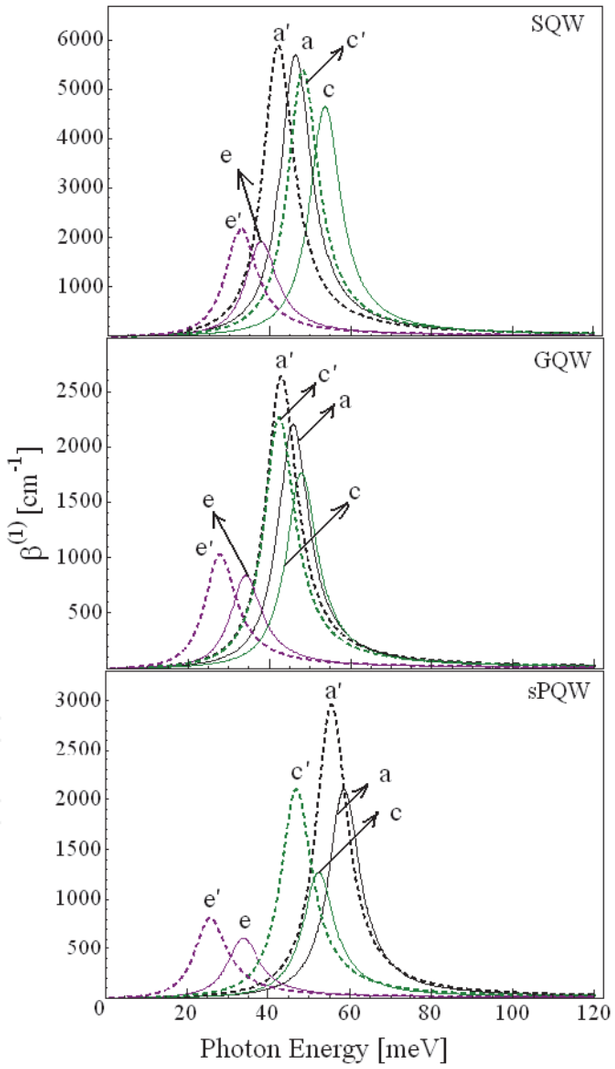

Fig. 7. Linear absorption coefficient, $\beta^{(1)}$, vs. pump photon energy in differently shaped n-sQWs with L_w = 150 Å under three laser intensities (same notations as in Fig. 1). L_c = 20 Å (solid lines) and 200 Å (dashed lines).

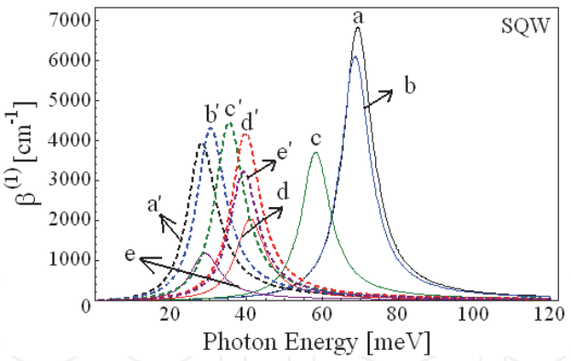

Fig. 8. Linear absorption coefficient, $\beta^{(1)}$, vs. pump photon energy in a n-sSQW with L_c = 50 Å under various laser dressing parameters. Notations a, b, c, d, and e stand for: α_0 = 0 (black), 20 Å (blue), 40 Å (olive), 60 Å (red), and 80 Å (purple), respectively. The QW widths are 100 Å (solid lines) and 200 Å (dashed lines).

In Fig. 9 the total absorption coefficient, $\beta(\omega_{ex}, I) = \beta^{(1)}(\omega_{ex}) + \beta^{(3)}(\omega_{ex}, I)$, as a function of the photon energy for different values of the incident optical intensity I, with and without applied laser field, in differently shaped n-sQWs having L_w = 150 Å and symmetrical barriers, is plotted. The cap layer thickness is L_c = 20 Å.

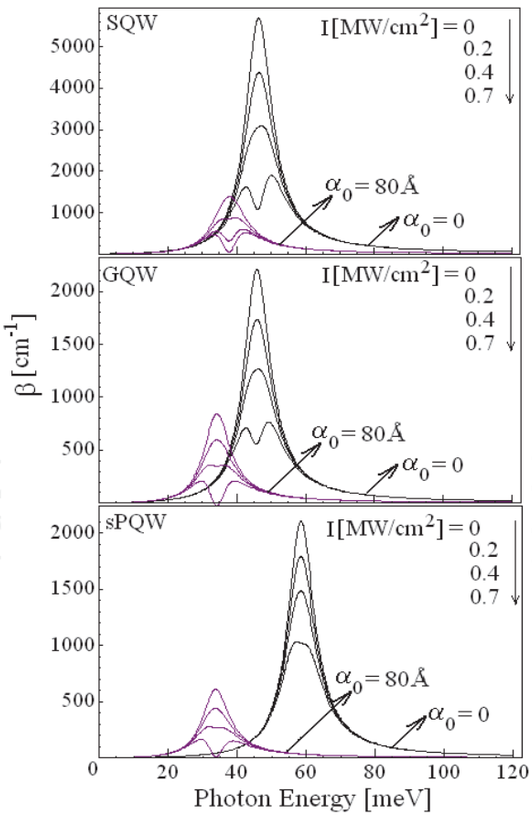

Fig. 9. Total absorption coefficient vs. pump photon energy in differently shaped n-sQWs with L_w = 150 Å, L_c = 20 Å and symmetrical barriers for two laser parameters α_0 = 0 (black) and 80 Å (purple). The vertical arrow indicates the rising of the exciting intensity.

The main findings for $\beta(\omega_{ex}, I)$ are:

i. there is no shift of the resonant peak positions with incident optical intensity, as expected;
ii. the total absorption coefficient β is significantly diminuted by the increasing optical intensity due to the negative nonlinear term, $\beta^{(3)}(\omega_{ex}, I)$. Therefore, both linear and nonlinear contributions should be taken into account in the calculated absorption coefficient β near the resonance frequency ($E_{tr} \cong \hbar\omega_{ex}$), especially for high exciting intensities.
iii. the magnitude peak of the total absorption coefficient is dramatically reduced by the intense laser field;
iv. the resonant peak of β can be bleached at sufficiently high incident optical intensities; the bleaching effect generates a split up of the resonant peak into two peaks. For our n-sQW structures the bleaching intensities depend on the confining potential shape, laser-dressing parameter, and cap layer thickness.

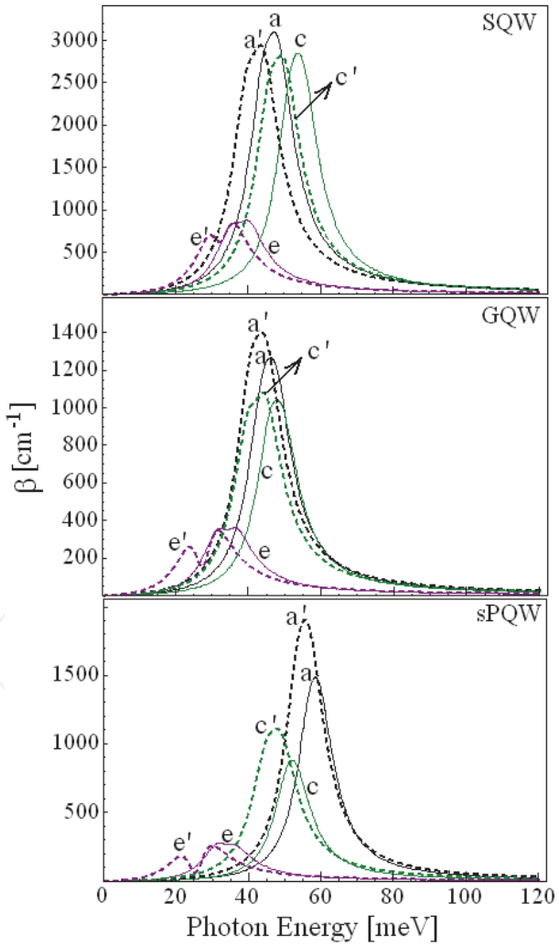

Fig. 10. Total absorption coefficient, $\beta = \beta^{(1)} + \beta^{(3)}$, vs. pump photon energy in differently shaped n-sQWs under the same conditions as in Fig. 7, and supplementary, with exciting intensity I = 0.4 MW/cm².

Similar results were reported for GaAs/AlGaAs uncapped QWs having different shapes: inverse V-type (Niculescu & Burileanu, 2010b) or graded-type (Ozturk, 2010).
In the particular case of a relatively low exciting intensity, I = 0.4 MW/cm², the dependence of the total absorption coefficient β on the laser-dressing parameter (Fig. 10) is similar with that for $\beta^{(1)}(\omega_{ex})$ (see Fig. 7). Therefore, the exciting intensity may be used to modulate the intersubband absorption.
Concluding, we note that the optical properties of the differently shaped n-sQWs could be tuned by proper tailoring of the heterostructure parameters (well shape and width, cap layer thickness, barrier asymmetry) and/or by varying the laser field intensity. The switch between the strong absorption and induced laser transparency regimes can be suitable for good performance optical modulators.

3. Interband transitions in near-surface QWs under intense laser field

Excitons play an important role in the optical properties of quantum wells. Compared to those in three-dimensional bulk semiconductors, the exciton binding energy and oscillator strength in QWs are considerably enhanced due to quantum confinement effect, so excitons in QWs are more stable.
The electronic and optical properties of the semiconductor QWs are significantly modified by applying intense high-frequency laser fields and this effect provides new degrees of freedom for technological applications.

3.1 Theory

Let us consider again the n-sQW structure described in the Section 2.1. According to the effective mass approximation, in the absence of the laser field, the exciton Hamiltonian is

$$H = H_{ez} + H_{hz} + \frac{P_{\perp}^2}{2M} + \frac{p_{\perp}^2}{2\mu} + U_{eh} \,. \tag{14}$$

Here

$$H_{jz} = -\frac{\hbar^2}{2m_{jz}^*}\frac{\partial^2}{\partial z_j^2} + V_j(z_j) + V_{self}(z_j) \tag{15}$$

are the single-particle 1D Hamiltonians. The symbol $j = e,h$ denotes the electron (hole) and V_j is the confinement potential in the growth direction (z-axis). The forms of V_j for the three n-sQWs are given by the Eqs. (3 a, b, and c), but V_0 must be replaced by V_e (for electron) and V_h (for hole). The last term in Eq. (15) represents the electrostatic energy of the repulsive interaction between the carriers and their image-charges

$$V_{self}(z_j) = \frac{e_0^2}{2\varepsilon}\left(\frac{\varepsilon - 1}{\varepsilon + 1}\right)\frac{1}{2d_{0j}} \,. \tag{16}$$

Here ε is the semiconductor dielectric constant, $e_0^2 = e^2/4\pi$, and d_{0j} is the distance between the electron (hole) and its image-charge. The third and fourth terms of Eq. (14) are the kinetic operators of the mass-center motion and relative motion of an exciton, respectively, in the (x-y) plane.

The last term in Eq. (14) describes the total electron-hole Coulomb interaction (Chang & Peeters, 2000) as

$$U_{eh}\left(\rho, z_e, z_h\right) = -\frac{e_0^2}{\varepsilon}\left[\frac{1}{\sqrt{\rho^2 + \left(z_e - z_h\right)^2}} + \left(\frac{\varepsilon - 1}{\varepsilon + 1}\right)\frac{1}{\sqrt{\rho^2 + d_{e-h}^2}}\right], \tag{17}$$

where ρ denotes the in-plane relative coordinate $\rho = \left|\boldsymbol{\rho}_e - \boldsymbol{\rho}_h\right|$; d_{e-h} is the distance between the electron (hole) and hole-image (electron-image) along the z-axis. For the sake of simplicity, in Eqs. (14–17) we have assumed that the electron and hole effective masses as well as the dielectric constant do not vary inside the whole heterostructure.

By applying a non-resonant intense laser field (ILF) which has the polarization direction parallel to the QW growth direction (z-axis), in the high-frequency limit (Marinescu & Gavrila, 1995), the electron (hole) "sees" a laser-dressed potential which is obtained by averaging the confining potential $V_j\left(z_j + \alpha_j(t)\right)$ over a period

$$\tilde{V}\left(z, \alpha_{0j}\right) = \frac{\omega_{LF}}{2\pi}\int_0^{2\pi/\omega_{LF}} V_j\left(z_j + \alpha_j(t)\right)dt. \tag{18}$$

The quantity

$$\alpha_j(t) = \alpha_{0j}\sin\left(\omega_{LF}\, t\right) \tag{19}$$

describes the motion of the electron (hole) in the laser field of frequency ω_{LF}; α_0 is the laser-dressing parameter, similar with that given by the Eq. (6), i.e. $\alpha_{0j} = eA_0 / \left(m_{jz}^* \omega_{LF}\right)$. The laser-dressed repulsive interaction between the carriers and their self-image charges can be approximated by a soft-core potential (Lima, C.A.S. & Miranda, 1981) as

$$\tilde{V}_{self}\left(z, \alpha_{0j}\right) = \frac{e_0^2}{4\varepsilon}\left(\frac{\varepsilon - 1}{\varepsilon + 1}\right)\frac{1}{\sqrt{d_{0j}^2 + \alpha_{0j}^2}} \tag{20}$$

Following some important studies (Gavrila & Kaminski, 1984; Lima, C.A.S. & Miranda, 1981; Marinescu & Gavrila, 1995) the dressed single-particle eigenstates are the solutions of time-independent Schrödinger equations

$$\left[-\frac{\hbar^2}{2m_{jz}^*}\frac{\partial^2}{\partial z_j^2} + \tilde{V}_j\left(z_j, \alpha_{0j}\right) + \tilde{V}_{self}\left(z_j, \alpha_{0j}\right)\right]\tilde{\varphi}_j\left(z_j\right) = E_j\tilde{\varphi}_j\left(z_j\right), \quad j = e, h\,. \tag{21}$$

In order to obtain the envelope wave functions and subband energies of both electron and hole in these modified potentials we have used a transfer matrix method (Ando & Ytoh, 1987; Tsu & Esaki, 1973).

Within the same approximation of the soft-core potential the dressed exciton binding energy was calculated by using the replacement

$$U_{eh}\left(\rho, z_e, z_h\right) \to -\frac{e_0^2}{\varepsilon}\left[\frac{1}{\sqrt{\rho^2 + \left(z_e - z_h\right)^2 + \alpha_0^2}} + \left(\frac{\varepsilon - 1}{\varepsilon + 1}\right)\frac{1}{\sqrt{\rho^2 + d_{e-h}^2 + \alpha_0^2}}\right] \tag{22}$$

in the Hamiltonian (14). In the Eq. (23) $\alpha_0 = eA_0 / (\mu\omega_{LF})$ is the laser parameter for the *exciton*. Assuming a strong quantization in the QW potentials the separate trial wave function for the ground exciton state (1S) is chosen (Miller, R.C. et al., 1981) as

$$\Psi_{ex} = N\tilde{\varphi}_e(z_e)\,\tilde{\varphi}_h(z_h)\,\chi(\rho,\lambda) \tag{23}$$

Here N is a normalization constant, while $\varphi_e(z_e)$ and $\varphi_h(z_h)$ are the ground state eigenfunctions of the laser-dressed Hamiltonians $\tilde{H}_{ez}$ and $\tilde{H}_{hz}$, respectively. These operators are obtained by replacing the Eqs. (18) and (21) in Eq. (15). $\chi(\rho,\lambda) = \exp(-\rho/\lambda)$ is a 2D hydrogenic function with λ as variational parameter. Then, the exciton binding energy is calculated as

$$E_b = E_e + E_h - \min_{\lambda} \frac{\langle \Psi_{ex} | H | \Psi_{ex} \rangle}{\langle \Psi_{ex} | \Psi_{ex} \rangle}, \tag{24}$$

where E_e and E_h are the single-particle energies of the electron and hole, respectively.

In order to systematically investigate the ILF effects on the optical n-sQW properties, the linear absorption coefficient of the excitonic transitions induced by an exciting light which is polarized along the *z*-direction have been calculated. We denote by ω_{ex} the angular frequency of the light from a tunable source. Assuming the dipole approximation, the absorption coefficient (Bassani & Parravicini, 1975) depends on the oscillator strength per unit area, *f*, as

$$\beta(\omega_{ex}) = \frac{4\pi^2 e^2 \hbar f}{n_r c m_0 L} \frac{\Gamma/2\pi}{(\hbar\omega_{ex} - E_{ex})^2 + (\Gamma/2)^2} \tag{25}$$

where the following notations were used: m_0 the free-electron mass, n_r the refractive index of the QW material, L the total thickness of the structure, $E_{ex} = E_{g\,well} + E_e + E_h - E_b$ the excitonic transition energy and Γ the linewidth.

On the other hand, the oscillator strength per unit area is connected to the excitonic wave function (Bassani & Parravicini, 1975) by

$$f = \frac{2M^2}{m_0 E_{ex}} \left| \langle \tilde{\varphi}_e(z_e) | \tilde{\varphi}_h(z_h) \rangle \right|^2 |\chi(0)|^2, \tag{26}$$

where M is the optical transition matrix element between the valence and conduction bands, $\varphi_j(z_j)$ are the single-particle wave functions under applied laser field, and $|\chi(0)|^2$ denotes the probability of finding the electron and hole at the same position. For the allowed optical transitions between the hh1 and e1 subbands we obtain

$$\beta(\omega_{ex}) = B \left| \langle \tilde{\varphi}_e(z_e) | \tilde{\varphi}_h(z_h) \rangle \right|^2 |\chi(0)|^2 \frac{\Gamma/2}{(\hbar\omega_{ex} - E_{ex})^2 + (\Gamma/2)^2} \tag{27}$$

where the quantity B is almost frequency-independent in the frequency range of the interband transitions (Bastard, 1981). So, B was taken as a constant.

3.2 Electronic properties

The numerical calculations were carried out for $In_{0.18}Ga_{0.82}As/GaAs$ differently shaped n-sQWs with the well width L_w = 50 Å or 80 Å and various cap layer thicknesses, L_c = 40 Å, 80 Å, 120 Å, by using the material parameters (Gippius et al., 1998) listed in Table 2 and a broadening parameter Γ = 1 meV (Sari et al., 2003). The chosen values for L_w and L_c allowed us to validate the calculation results by the reported experimental data (Gippius et al., 1998; Kulik et al., 1996; Li, Z. et al., 2010; Yablonskii et al., 1996).

Material	GaAs	$In_{0.18}Ga_{0.82}As$
V_e (meV)	113	0
V_h (meV)	75	0
m_e/m_0	0.067	0.067
m_{hz}/m_0	0.35	0.35
$m_{h\perp}/m_0$	0.112 *	0.112 *
E_g^Γ (meV)	1519	1331
ε_s	12.5	12.5
ε_∞	10.9	10.9

Table 2. Material parameters used in calculations. (*Maialle & Degani, 2001)

For two nanostructures, GQW and sPQW, one of the GaAs barriers (the cap layer) has an unchanged height, V_e (electron) or V_h (hole), and the other barrier is variable, $V_r = \sigma V_{e/h}$. The following values for the asymmetry parameter have been used: σ = 0.6, 0.8, and 1. The SQW structure is a symmetrical one (σ = 1). The laser parameter was chosen in the range of ILF, i. e. $\alpha_0 \in [0, 120\ \text{Å}]$.

3.2.1 Single-particle energies

The strong laser effect on the potential profile and on energy levels of the conduction band (CB) for SQW, GQW and sPQW with L_w = 150 Å was discussed in the Section 2.2.1. For narrower n-sQWs with L_w = 50 Å or 80 Å the main laser-induced properties of the CB are very similar (Eseanu, 2011; Niculescu & Eseanu, 2011). In contrast, the laser parameter augmentation has little effect on the heavy-hole potential (not plotted here) because $\alpha_0 \propto 1/m^*$ (see Eq. (20) and Table 2).

In Figs. 11A and 11B the single-particle electron and hole energies, respectively, are plotted as functions of the laser intensity, α_0, in three differently shaped n-sQWs with L_c = 40 Å, for several values of the asymmetry parameter: σ = 0.6, 0.8, and 1.

We can see that the ground state energy in the conduction band first rapidly raises with the laser parameter up to $\alpha_0 \cong 40$ Å, i. e. $\alpha_0 = L_w/2$, and for further large laser intensities the E_e-level becomes less sensitive to the laser field (Fig. 11A). This is a typical behavior for low-dimensional systems under ILFs, as mentioned in Section 2.2.1. Instead, the valence band states (Fig. 11B) are less affected by the radiation field because of the weaker change of the laser-dressed confinement potential, in comparison with the electronic potential.

The values of the single-particle energies are greater in sPQW than in GQW due to the stronger geometric confinement. Also, the increasing of the barrier asymmetry, σ, generates an enhancement of the energy levels of both electrons and holes in GQW and sPQW (Figs.

11 A, B), as expected. For example, the electronic energies increase almost linearly with σ, as the inset of Fig. 11A shows.

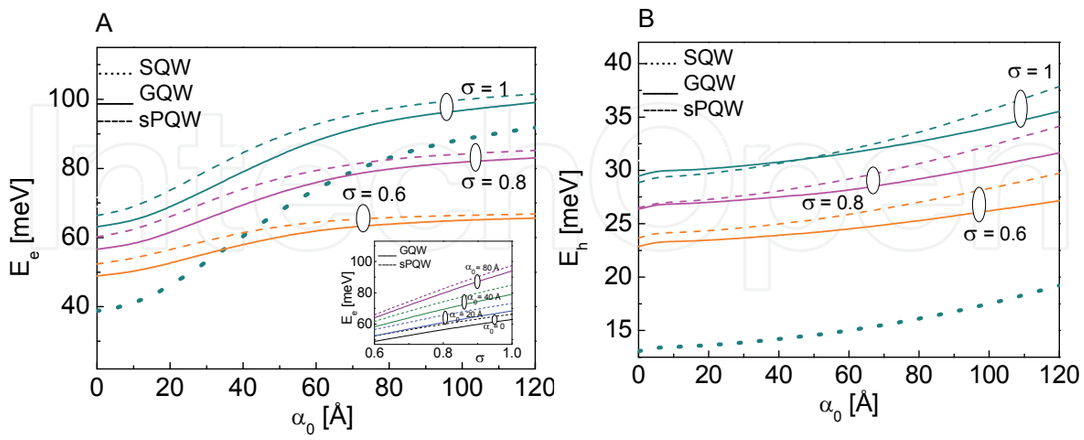

Fig. 11. The single-particle energy of the electron (A) and hole (B) as functions of the laser intensity, α_0 , in three differently shaped n-sQWs with L_c = 40 Å, for various asymmetry parameter values: σ = 0.6 (orange), 0.8 (magenta), and 1 (dark cyan). Inset A: the electronic energy vs. the asymmetry parameter for GQW and sPQW under different laser intensities.

The single-particle electron and hole energies are significantly modified by the capped layer thickness as Figs. 12 A, B prove for two types of n-sQWs with L_w = 50 Å and identical barriers, under different laser intensities.

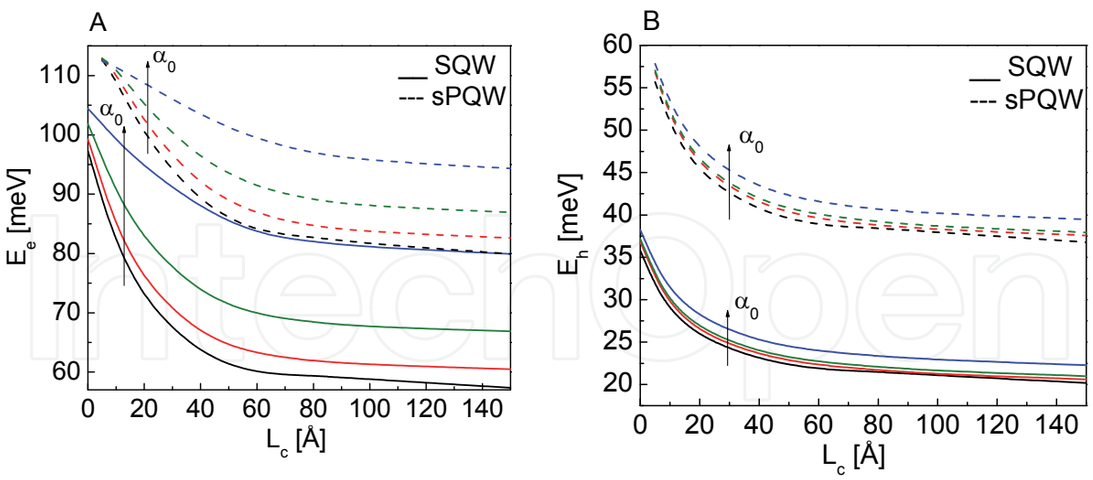

Fig. 12. The single-particle energy for electron (A) and hole (B) vs. capped layer thickness under different laser field intensities: α_0 = 0 (black), 10 Å (blue), 20 Å (olive), and 40 Å (red) for two types of n-sQWs with L_w = 50 Å and identical barriers.

It can be seen that the ground state energy in the conduction band first rapidly decreases with cap layer up to $L_c \cong$ 50 Å, and for further thick cap layers it becomes insensitive to the dielectric enhancement. For thin cap layers, the stronger geometric confinement of the

electron in the sPQW comparing with SQW leads to an enhanced shift of the E_e-level toward higher energies. Also, the electron energy presents a significant laser-induced augmentation which is more pronounced for sPQWs with thicker cap layer. There are two reasons for this behavior:

i. as the cap layer thickness increases the contribution of the image-charge is weakened and the ILF effect becomes dominant;
ii. under laser field action, the potential profile of SQW changes faster than in sPQW, so that the ground state of square structure are faster moved up in the upper part of the dressed QW.

In contrast, the valence band states are less affected by the radiation field. With the decrease of L_c the contribution of dielectric confinement to the hole energy becomes dominant leading to a pronounced blueshift. This result are in good agreement with the previous theoretical and experimental data in the absence of the laser field (Gippius, 1998; Tran Thoai, 1990).

3.2.2 Exciton binding energy

A noticeable dependence of the electron-hole interaction on the laser parameter, α_0, is expected as a consequence of the obvious laser-induced modification in the electronic structure of the CB. Fig. 13 displays the 1S-exciton binding energy as a function of the laser parameter for SQW, GQW and sPQW with L_c = 40 Å and different barrier asymmetries. We observe that for all the heterostructures under our study the exciton binding energy, E_b, first increases with α_0, reaches a maximum value at $\alpha_0 \cong 6$ Å, and then it experiences a pronounced diminution. Finally, for large enough laser amplitudes E_b drops to the $In_{0.18}Ga_{0.82}As$ bulk characteristic value, 4.45 meV (Chang & Peeters, 2000). In the range of our calculations this value is reached for the sPQW with σ = 0.6 under intense laser field, α_0 = 120 Å.

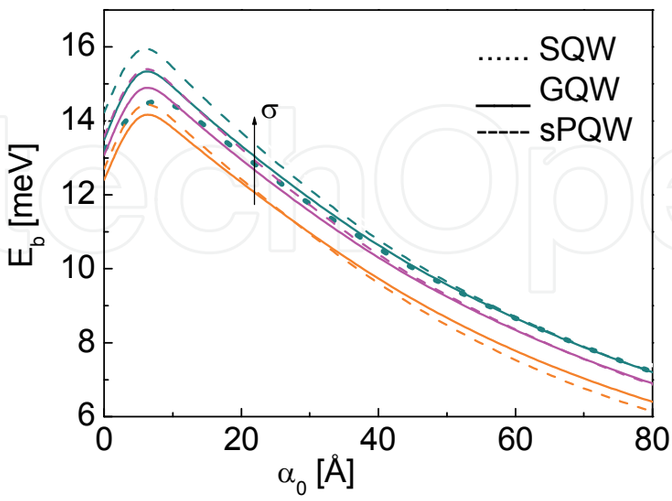

Fig. 13. The exciton binding energy vs. the laser-field intensity in three differently shaped n-sQWs: SQW (doted line), GQW (solid lines) and sPQW (dashed lines) with L_c = 40 Å and various asymmetry parameter values (the same as in Fig. 11).

The explanation of this behavior may be the following: under a low laser field ($\alpha_0 <$ 10 Å) the electronic ground level is localized in the lower part of the dressed QW which has a narrow width; therefore, the small distance between the electron and hole leads to a considerable exciton binding energy. By increasing the laser field intensity the geometric confinement of the carriers is reduced and thus, they can easily penetrate into the QW barriers. This "travel" results in a pronounced diminution of E_b .

As the barrier asymmetry parameter, σ, increases the exciton binding energy is enhanced due to the higher right barrier ($V_r = \sigma V_{e/h}$) which moderates the spreading of the carriers wavefunctions in the QW barriers. Therefore, under intense laser field a competition between the laser intensity and barrier asymmetry in "tailoring" the exciton binding energy occurs.

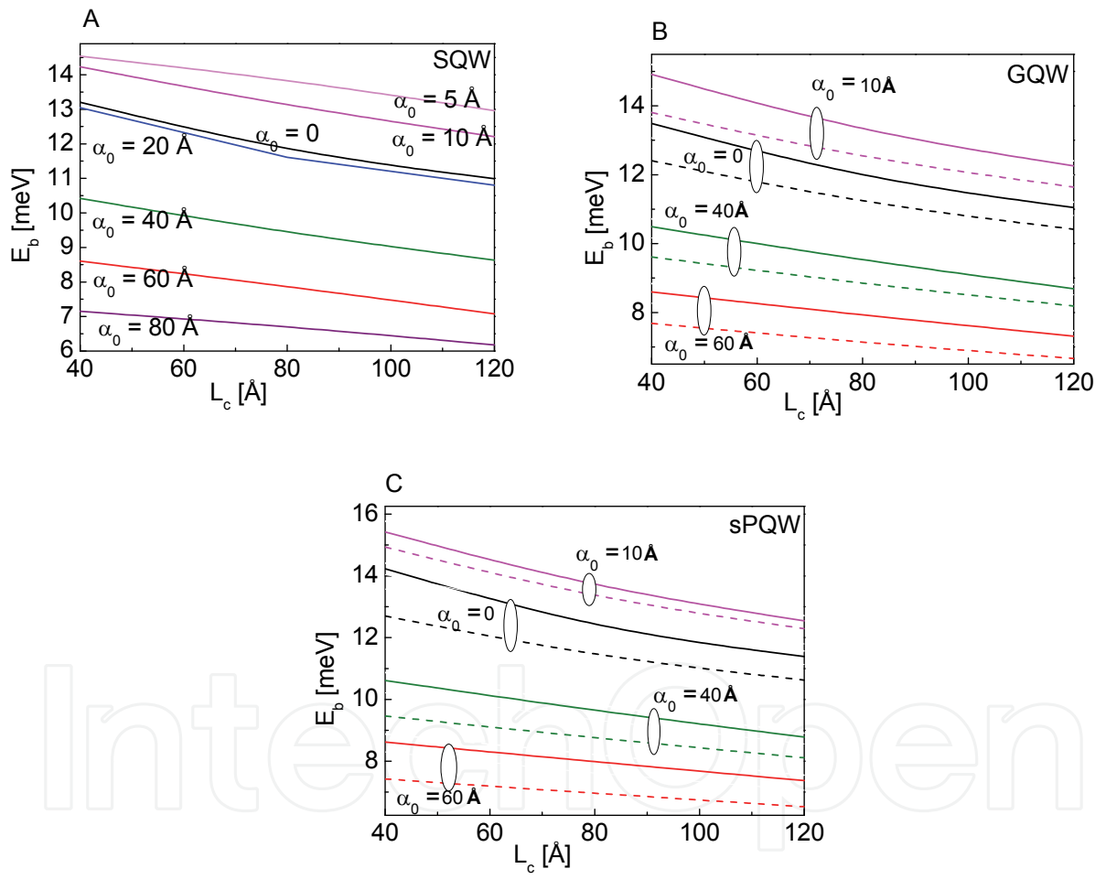

Fig. 14. The exciton binding energy vs. the cap layer thickness in three differently shaped n-sQWs with L_c = 40 Å, for two asymmetry parameter values: σ = 0.6 (dashed lines) and 1 (solid lines) under different laser field intensities α_0 : 0 (black), 5 Å (light magenta), 10 Å (magenta), 20 Å (blue), 40 Å (olive), 60 Å (red) and 80 Å (purple); A) SQW, B) GQW and C) sPQW.

In Figs. 14 A-C the exciton binding energy is plotted as a function of the cap layer thickness, L_c , in three differently shaped n-sQWs under various laser field intensities. For the

asymmetrical structures GQW and sPQW two values of the asymmetry parameter, σ = 0.6 and 1, were used.

We observe that for $L_c \geq$ 40 Å and for all laser parameter values used in this work, the exciton binding energy in the three differently shaped n-sQWs is reduced as L_c increases. A similar behavior has been reported for a square n-sQW with L_w = 50 Å in two cases: i) under various laser intensities (Niculescu & Eseanu, 2010a) and ii) in the absence of the laser field (Kulik et al., 1996). This dielectric enhancement of E_b obtained by using narrow capped layers, which are experimentally available, could be exploited in new optoelectronic devices.

The exciton binding energy properties (presented above) reveal the transition from two-dimensional confinement effect produced by the wave function squeezing in a symmetrical/asymmetrical InGaAs quantum well to the three-dimensional behavior of the exciton, as α_0 increases. A similar variation of the ground state binding energy has been reported for excitons in quantum well wires (Sari et al., 2003) and in n-sQWs with symmetrical barriers (Niculescu & Eseanu, 2011), under intense laser field.

3.3 Exciton absorption spectra

The exciton absorption coefficient given by the Eq. (27) depends on the exciton transition energy, E_{ex}, whose components have been discussed in Section 3.2 and on the overlap integral $\left|\left\langle \tilde{\varphi}_e(z_e)\middle|\tilde{\varphi}_h(z_h)\right\rangle\right|^2$. Figs. 15 A, B display the simultaneous dependence of this overlap on the cap layer thickness and laser field parameter in two n-sQWs (SQW and sPQW) with L_w = 50 Å and identical barriers. As expected, this quantity decreases with α_0, especially in SQW, due to laser-induced spreading of the carriers wave functions in the dressed n-sQW barriers.

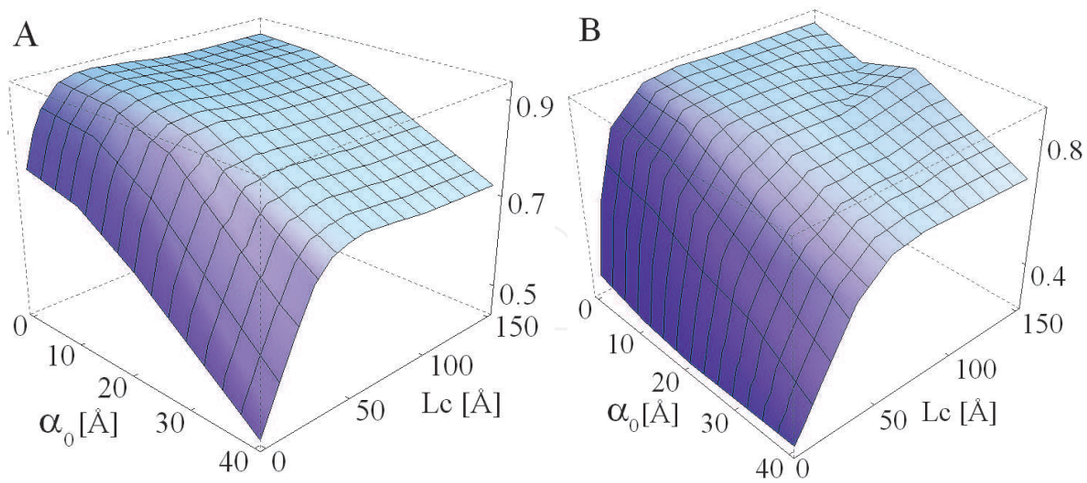

Fig. 15. The dependence of the overlap integral on the cap layer thickness, L_c, and laser field intensity, α_0 in two n-sQWs: A) SQW and B) sPQW with L_w = 50 Å and identical barriers.

We can also observe that, if α_0 is kept unchanged, there is an optimal range of the cap layer thickness corresponding to a broad maximum of the overlap integral. As α_0 increases this

optimal range is shifted to larger L_c values in SQW, whereas it remains practically unchanged in the stronger confining structure sPQW. Moreover, since in the sPQW the particles are mostly localized in the QW region, the average electron-hole distance is less sensitive to the laser amplitude leading to an overlap integral nearly independent on the α_0 values.

Fig. 16 displays the overlap dependence on the barrier asymmetry parameter and laser field intensity in an asymmetrical n-sQW, namely GQW with L_c = 80 Å. The intense laser field reduces the overlap, as discussed before. Instead, the overlap integral is enhanced by the increasing barrier asymmetry (σ), particularly in low laser fields ($\alpha_0 \leq$ 40 Å). A similar variation was obtained for sPQW having the same L_c = 80 Å (not plotted here).

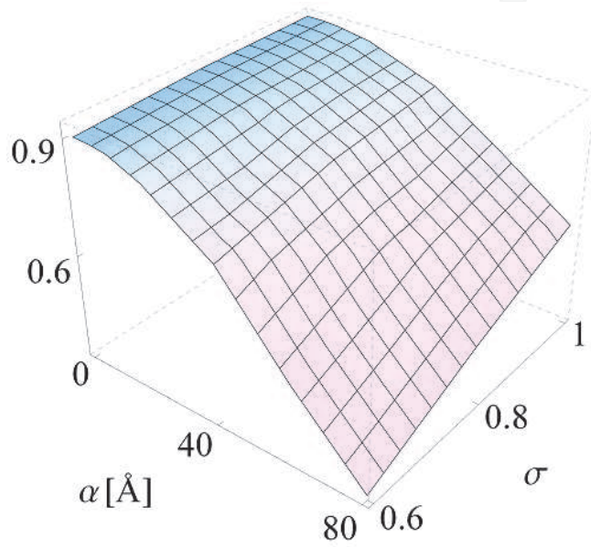

Fig. 16. The dependence of the overlap integral on the barrier asymmetry parameter, σ, and laser field intensity, α_0 in an asymmetrical n-sQW, namely GQW with L_c = 80 Å.

This asymmetry effect can be explained by the spreading effect of the wave functions in a QW with reduced barriers. The increasing of the height barrier in the QW right side ($V_r = \sigma V_{e/h}$) in joint action with a low laser field lead to a stronger localization of the wave functions inside the well. Again, the intense laser field action competes with the asymmetry parameter, in the present case on the overlap integral. This effect could be used for particular applications.

The exciton absorption coefficient (EAC) is modified by several parameters: pump photon energy, capped layer thickness L_c, laser intensity α_0, and barrier asymmetry σ. In Figs. 17 A, B the dependence of this quantity vs. the pump photon energy in differently shaped n-sQWs with L_w = 80 Å, under various laser intensities α_0 = 0, 20 Å , 40 Å, and 60 Å, is plotted as follows: a) for SQW with identical barrier heigths and different L_c (Fig. 17A); b) for GQW and sPQW having two asymmetry parameter values (Fig. 17 B).

Firstly, one can see that the increasing laser intensity generates a significant shift of the absorption peak position to the high photon energies (blue-shift) and a simultaneous reduction of the exciton absorption coefficient magnitude, for all the cases under our study.

A similar effect was observed for square and semiparabolic n-sQWs of the same width L_w = 50 Å, having identical barrier heights and variable cap layer thickness (Niculescu & Eseanu, 2011). As expected, the shifts of the EAC peaks are more pronounced in the SQW (Fig. 17A) due to the weaker quantum confinement afforded by this structure in comparison with GQW and sPQW.

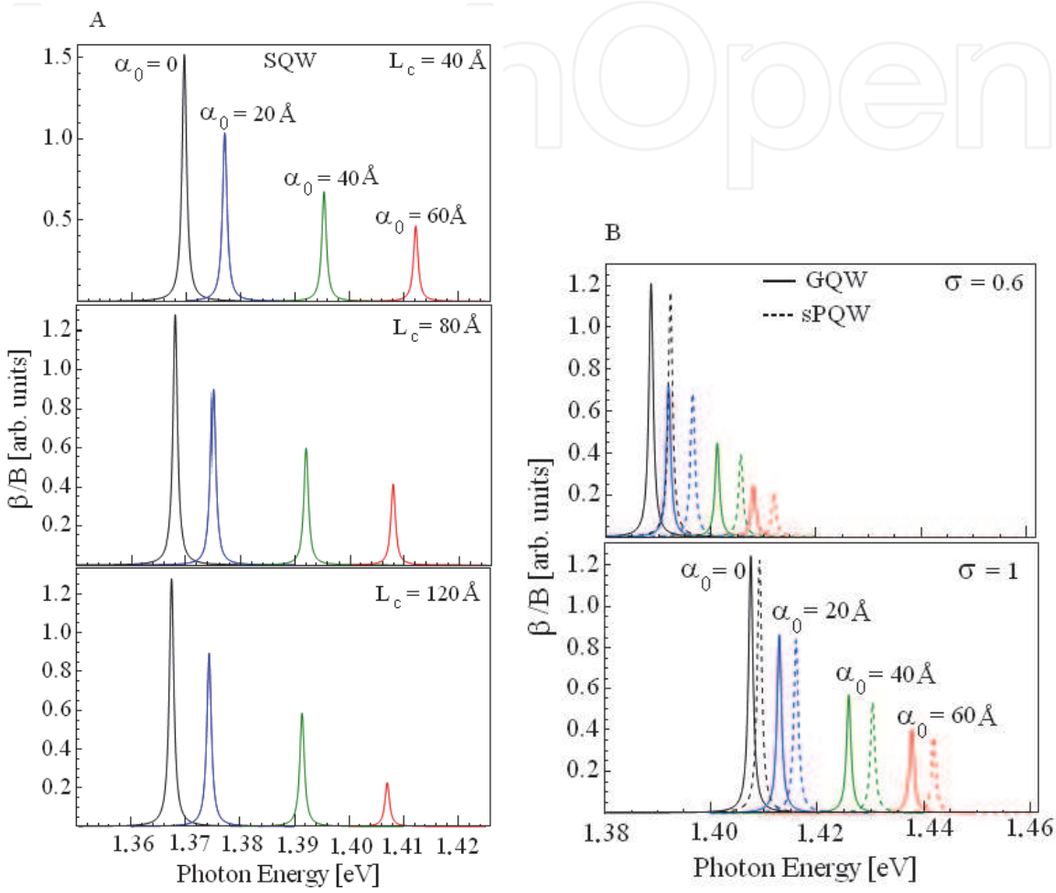

Fig. 17. The exciton absorption coefficient as a function of the pump photon energy in: A) SQW for three values of the cap layer thickness; B) GQW (solid lines) and sPQW (dashed lines) for two barrier asymmetries, under various laser intensities α_0 = 0 (black), 20 Å (blue), 40 Å (olive), 60 Å (red).

The reason for the EAC laser-induced reduction is two-fold:

i. the overlap integral diminution under intense laser fields (Figs. 15, 16);
ii. the typical laser-induced blue-shift of the E_e-levels.

Secondly, we observe that the EAC peak positions show a red-shift for thicker cap layers (in the range 40 Å - 80 Å) whereas for $L_c > 80$ Å these positions are insensitive to the cap layer variation.

Thirdly, we note that in the asymmetrical n-sQWs (GQW and sPQW) the blue-shift of the exciton absorption peak positions for σ = 1 (identical barriers) is more pronounced comparing with the case σ = 0.6.

For the $In_{0.18}Ga_{0.82}As/GaAs$ near-surface SQW with L_w = 50 Å and variable L_c, in the absence of the laser field, our results (Niculescu & Eseanu, 2010a) agree with the photoluminescence excitation measurements (Gippius et al., 1998; Kulik et al., 1996; Li, Z. et al., 2010; Yablonskii et al., 1996) and with theoretical normal-incidence reflectivity spectra (Yu et al., 2004).

It is important to emphasize that the red-shift induced by the increasing L_c or by the decreasing σ can be effectively compensated using the blue-shift caused by the enhanced laser parameter. The changes induced by the joint action of the laser intensity and capped layer thickness or barrier asymmetry parameter in differently shaped QWs can be exploited to design new optoelectronic devices.

4. Conclusion

Summarizing, we note that the optical properties of the $In_{0.18}Ga_{0.82}As/GaAs$ differently shaped near-surface quantum wells under intense laser fields could be tuned by proper tailoring of the heterostructure parameters (well shape and width, cap layer thickness, barrier asymmetry) and/or by varying the laser field intensity. This characteristics holds for both intersubband and interband absorptions. For example, in the exciton spectra of narrow $In_{0.18}Ga_{0.82}As/GaAs$ n-sQWs, our calculations show that the red-shift of the absorption peaks induced by the rising cap layer thickness or by barrier asymmetry diminution can be effectively compensated using the blue-shift caused by enhancing laser parameter. These phenomena could be exploited for particular applications. Also, for both intersubband and interband transitions, the switch between the strong absorption and induced laser transparency regimes can be suitable for good performance optical modulators.

To the best of our knowledge this is the first investigation on the intersubband absorption in symmetrical/asymmetrical InGaAs/GaAs n-sQWs under intense laser fields. We expect that these results will be of help for experimental works focused on innovative optoelectronic devices.

5. Acknowledgement

The author would like to express her special thanks to Professor E. C. Niculescu for helpful discussions and constant support.

6. References

Ahn, D. & Chuang, S.L. (1987). Intersubband optical absorption in a quantum well with an applied electric field. *Phys. Rev. B*, vol. 35, No. 8, (1987), 4149-4151, ISSN 1098-0121.

Alves, F.D.P.; Karunasiri, G.; Hanson, N.; Byloos, M.; Liu, H.C.; Bezinger, A. & Buchanan, M. (2007). NIR, MWIR and LWIR quantum well infrared photodetector using interband and intersubband transitions. *Infrared Phys. & Technol.* vol. 50, No. 2-3, (April 2007), 182-186, ISSN 1350-4495.

Ando, Y. & Ytoh, T. (1987). Calculation of transmission tunneling current across arbitrary potential barriers . *J. Appl. Phys.* vol. 61, No. 4, (1987),1497-1502, ISSN 1089-7550.

Andreani, L.C. & Pasquarello, A. (1990). Accurate theory of excitons in $GaAs-Ga_{1-x}Al_xAs$ quantum wells. *Phys. Rev. B*, vol. 42, No. 14, (1990), 8928-8938, ISSN 1098-0121.

Asano, T.; Noda, S. & Sasaki, A. (1998). Absorption magnitude and phase relaxation time in short wavelength intersubband transitions in InGaAs/AlAs quantum wells on

GaAs substrates. *Physica E: Low-dimensional Systems and Nanostructures,* vol. 2, No. 1-4, (July 1998), 111-115, ISSN 1386-9477.

Bassani, F. & Parravicini, G. P. (1975). *Electronic States and Optical Transitions in Solids*; Pergamon: Oxford, 1975, Ch.5, ISBN 0080168469.

Bastard, G. (1981). Hydrogenic impurity states in a quantum well: A simple model. *Phys. Rev. B*, vol. 24, No. (1981), 4714-4722, , ISSN 1098-0121.

Bedoya, M. & Camacho, A.S. (2005). Nonlinear intersubband terahertz absorption in asymmetric quantum well structures. *Phys. Rev. B*, vol. 72, No. 15, (2005), 155318, ISSN 1098-0121.

Belkin, M.A.; Capasso, F.; Xie, F.; A. Balyanin, A.; Fischer, M.; Whitmann, A. & Faist, J. (2008). Room temperature terahertz quantum cascade laser source based on intracavity difference-frequency generation. *Appl. Phys. Lett.,* vol. 92, No. 20, (2008), 201101, ISSN 1077-3118.

Brandi, H. S.; Latge, A. & Oliveira, L. E. (2001) Dressed-band approach to laser-field effects in semiconductors and quantum-confined heterostructures. *Phys. Rev. B*, vol. 64, No. (2001), 035323... ISSN 1098-0121.

Carter, S.G.; Ciulin, V.; Sherwin, M.S.; Hanson, M.; Huntington, A.; Coldren, L.A. & Gossard, A.C. (2004). Terahertz electro-optic wavelength conversion in GaAs quantum wells: Improved efficiency and room-temperature operation. *Appl. Phys. Lett.* vol. 84, No. 6, (2004), 840-842, ISSN 1077-3118.

Chakraborty, T. & Apalkov, V. M. (2003). Quantum cascade transitions in nanostructures. *Adv. Phys.,* vol. 52 No. 5, (2003), 455-521, ISSN 1460-6976.

Chang, K. & Peeters, F. M. (2000) Asymmetric Stark shifts in $In_{0.18}Ga_{0.82}As/GaAs$ near-surface quantum wells: The image-charge effect. *J. Appl. Phys.* vol. 88, No. 9, (2000), 5246-5251, ISSN 1089-7550.

Chui, H.C.; Martinet, E.L.; Fejer, M.M. & Harris, J.S. (1994). Short wavelength intersubband transitions in InGaAs/AIGaAs quantum wells grown on GaAs. *Appl. Phys. Lett.*, vol. 64, No. 6, (Febr. 1994), 736-, ISSN 1077-3118.

Diniz Neto, O. O. & Qu, F. (2004). Effects of an intense laser field radiation on the optical properties of semiconductor quantum wells. *Superlatt. Microstruct.*, vol. 35, No. 1-2, (Jan-Febr. 2004), 1-8, ISSN 0749-6063.

Duque, C.A.; Kasapoglu, E.; Sakiroglu, S.; Sari H. & Sökmen, I. (2011). Intense laser effects on nonlinear optical absorption and optical rectification in single quantum wells under applied electric and magnetic field. *Appl. Surf. Sci.,* vol. 157, No. 6, (Jan. 2011), 2313-2319, ISSN 0169-4332.

Elsaesser, T. (2006). Ultrafast Dynamics of Intersubband Excitations in Quantum Wells and Quantum Cascade Structures, in Paiella, R. *Intersubband Transitions in Quantum Structures*, McGraw-Hill Companies, ISBN 0-07-145792-5, pp. 137-140.

Eseanu, N.; Niculescu, E. C. & Burileanu, L. M. (2009). Simultaneous effects of pressure and laser field on donors in $GaAs/Ga^{1-x}Al^{x}As$ quantum wells. *Physica E: Low-dimens. Syst. Nanostruct.,* vol. 41, No. 8, (Aug. 2009), 1386-1392, ISSN:1386-9477.

Eseanu, N. (2010). Simultaneous effects of laser field and hydrostatic pressure on the intersubband transitions in square and parabolic quantum wells. *Phys. Lett. A*, vol. 374, No. 10, (Febr. 2010), 1278- 1285, ISSN 0375-9601.

Eseanu, N. (2011). Intense laser field effect on the interband absorption in differently shaped near-surface quantum wells, *Phys. Lett. A,* vol. 375, No. 6 , (Febr. 2011), 1036-1042, ISSN 0375-9601.

Faist, J.; Capasso, F.; Sivco, D.L.; Sirtori, C.; Hutchinson, A.L. & Cho, A.Y. (1994). Quantum Cascade Laser. *Science,* vol. 264, No. 5158, (Apr. 1994), 553-556, ISSN 1095-9203.

Gavrila, M. & Kaminski, J. Z. (1984). Free-free transitions in intense high-frequency laser fields. *Phys. Rev. Lett.*, vol. 52, No. 8, (1984), 613-616, , ISSN 0031-9007.

Gippius, N. A.; Yablonskii, A. L.; Dzyubenko, A. B.; Tikhodeev, S. G.; Kulik, L. V.; Kulakovskii, V. D. & Forchel, A. (1998). Excitons in near-surface quantum wells in magnetic fields: Experiment and theory. *J. Appl. Phys.* vol. 83, No. 10, (1998), 5410-5417, ISSN 1089-7550.

Gunapala, S.D.; Bandara, K.S.M.V.; Levine, B.F.; Sarusi, G.; Park, J.S.; Lin,T.L.; Pike, W.T. & Liu, J.K. (1994). High performance InGaAs/GaAs quantum well infrared photodetectors. *Appl. Phys. Lett.* vol. 64, No. 25, (1994), 3431-3433, ISSN 1077-3118.

Helm, M. (2000). The Basic Physics of Intersubband Transitions, in *Intersubband Transitions in Quantum Wells:*

Physics and Device Applications I, Capasso, F. and Liu, H. C. (eds.), *Semiconductors and Semimetals*, vol. 62, 1-32 and 73-80, Academic Press, ISBN 0-12-752171-2, San Diego, USA.

Iizuka, N.; Kaneko, K. & Suzuki, N. (2006). All-optical switch utilizing intersubband transition in GaN quantum wells. *IEEE J. Quantum Electr.,* vol. 42, No. 8, (Aug. 2006), 765-771, ISSN 0018-9197.

Jho, Y. D.; Wang, X.; Reitze, D. H.; Kono, J.; Belyanin, A. A.; Kocharovsky, V. V.; Kocharovsky, Vl. V. & Solomon, G. S. (2010). Cooperative recombination of electron-hole pairs in semiconductor quantum wells under quantizing magnetic fields. *Phys. Rev. B*, vol. 81, No. 15 (2010), 155314, ISSN 1098-0121.

Karabulut, I.; Atav, U.; Safak, H. & Tomak, M. (2007). Linear and nonlinear intersubband optical absorptions in an asymmetric rectangular quantum well. *Eur. Phys. J. B,* vol. 55, No. 3, (Febr. I, 2007), 283-288 ISSN1434-6036.

Kasapoglu E. & Sökmen, I. (2008). The effects of intense laser field and electric field on intersubband absorption in a double-graded quantum well. *Physica B: Condensed Matter,* vol. 403, No. 19-20, (Oct. 2008), 3746-3750, ISSN 0921-4526.

Kramers, H. (1956). *Collected Scientific Papers,* North-Holland, Amsterdam, 1956, p. 866.

Kulik, L. V.; Kulakovskii, V. D.; Bayer, M.; Forchel, A.; Gippius, N. A. & Tikhodeev, S. G. (1996). Dielectric enhancement of excitons in near-surface quantum wells. *Phys. Rev. B* vol. 54, No. 4, (1996) R2335- R2338, ISSN 1098-0121.

Levine, B. F. (1993). Quantum-well infrared photodetectors. *J. Appl. Phys.*, vol. 74, No. 8, (1993), R1-R81, ISSN 1089-7550.

Li, J.; Choi, K.K.; Klem, J.F.; Reno, J.L. & Tsui, D.C. (2006). High gain, broadband InGaAs/InGaAsP quantum well infrared photodetector. *Appl. Phys. Lett.* vol. 89, No. 8, (2006), 081128, ISSN 1077-3118.

Li, S.S. (2002). Multi-color, broadband quantum well infrared photodetectors for mid-, long-, and very long wavelength infrared applications. *International Journal of High Speed Electronics and Systems*, vol. 12, No. 3, (2002), 761-801, ISSN 0129-1564.

Li, Y.; Bhattacharya, A.; Thomodis, C.; Moustakas, T.D. & Paiella, R. (2007). Ultrafast all-optical switching with low saturation energy via intersubband transitions in GaN/AlN quantum-well waveguides. *Opt. Express*, vol.15, No. 26, (2007), 17922-17927, ISSN 1094-4087.

Li, Z. ; Wu, J.; Wang, Z. M.; Fan, D.; Guo A.; Li, S.; Yu, S. Q.; Manasreh O.; & Salamo, G. J. (2010). InGaAs Quantum Well Grown on High-Index Surfaces for Superluminescent Diode Applications, *Nanoscale Res. Lett.* vol. 5, No. 6, (2010),1079-1084, ISSN 1556-276X.

Lima, C. A. S. & Miranda, L. C. M. (1981). Atoms in superintense laser fields. *Phys. Rev. A*, vol. 23, No. 6, (1981), 3335-3337, ISSN 1050-2947.

Lima, F. M. S.; Amato, M. A.; Nunes, O. A. C.; Fonseca, A. L. A.; Enders, B. G. & Da Silva Jr., E. F. (2009). Unexpected transition from single to double quantum well potential induced by intense laser fields in a semiconductor quantum well. *J. Appl. Phys.*, vol. 105, No. (2009), 123111, ISSN 1089-7550.

Liu, H.C. (2000). Quantum well infrared photodetector physics and novel devices, in *Intersubband Transitions in Quantum Wells: Physics and Device Applications I,* Capasso, F. and Liu, H. C. (eds.), *Semiconductors and Semimetals*, vol. 62, 129-196, Academic Press, ISBN 0-12-752171-2, San Diego, USA

Maialle, M. Z. & Degani, M. H. (2001). Transverse magnetic field effects upon the exciton exchange interaction in quantum wells. *Semicond. Sci. Technol.*, vol. 16, No. (2001), 982-985, ISSN .

Marinescu, M. & Gavrila, M. (1995). First iteration within the high-frequency Floquet theory of laser-atom interactions. *Phys. Rev. A*, vol. 53, No. 4, (1995), 2513-2521, ISSN 1094-1622.

Miller, D.A.B.; Chemla, D.S. & Schmitt-Rink, S. (1986). Relation between electroabsorption in bulk semiconductors and in quantum wells: The quantum-confined Franz-Keldysh effect. *Phys. Rev. B*, vol. 33, No. 10, (1986), 6976-6982 , ISSN 1098-0121.

Miller, R. C.; Kleinman, D. A.; Tsang, W. T. & Gossard, A. C. (1981). Observation of the excited level of the excitons in GaAs quantum wells. *Phys. Rev. B*, vol. 24, No. 2, (1981), 1134-1136, ISSN 1098-0121.

Niculescu, E. C. & Eseanu N. (2010a) Dielectric enhancement of the exciton energies in laser dressed near-surface quantum wells. *Superlatt. Microstruct.*, vol. 48, No. 4, (Oct. 2010), 416-425, ISSN 0749-6063.

Niculescu, E. C. & Burileanu, L.M. (2010b). Nonlinear optical absorption in inverse V-shaped quantum wells modulated by high-frequency laser field. *Eur. Phys. J. B*, vol. 74, No. 1, (March I, 2010), 117-122, ISSN 1434-6036.

Niculescu, E. C. & Radu, A. (2010c). Laser-induced diamagnetic anisotropy of coaxial nanowires. *Curr. Appl. Phys.*, vol. 10, No. 5, (2010), 1354-1359, ISSN 1567-1739.

Niculescu, E. C. & Eseanu N. (2011). Interband absorption in square and semiparabolic near-surface quantum wells under intense laser field. *Eur. Phys. J. B*, vol. 79, No. 3, (Febr. I, 2011), 313-319, ISSN 1434-6036.

Noda, S.; Uemura, T.; Yamashita, T. & Sasaki, A. (1990). All-optical modulation using an *n*-doped quantum-well structure. *J. Appl. Phys.* vol. 68, No. 12, (1990), 6529-6531, ISSN 1089-7550.

Ozturk, E.; Sari H. & Sokmen I. (2004). The dependence of the intersubband transitions in square and graded QWs on intense laser fields. *Solid State Comm.,* vol. 132, No. 7, (Nov. 2004), 497-502, ISSN*:* 0038-1098.

Ozturk, E.; Sari H. & Sokmen I. (2005). Electric field and intense laser field effects on the intersubband optical absorption in a graded quantum well. *J. Phys. D: Appl. Phys.,* vol. 38, No. 6, (2005), 935-941, ISSN 1361-6463.

Ozturk, E. (2010). Nonlinear optical absorption in graded quantum wells modulated by electric field and intense laser field. *Eur. Phys. J. B*, vol. 75, No. 2, (2010), 197-203, ISSN 1434-6036.

Passmore, B. S.; Wu, J.; Manasreh, M. O. & Salamo, G. J. (2007). Dual broadband photodetector based on interband and intersubband transitions in InAs quantum dots embedded in graded InGaAs quantum wells. *Appl. Phys. Lett.*, vol. 91, No. 23, (2007), 233508, ISSN 1077-3118.

Rosencher, E. & Bois, Ph. (1991). Model system for optical nonlinearities: Asymmetric quantum wells. *Phys. Rev. B*, vol. 44, No. 20, (1991), 11315-11327, ISSN 1098-0121.

Sari, H.; Kasapoglu, E.; Sokmen, I. & Gunes, M. (2003). Optical transitions in quantum well wires under intense laser radiation. *Phys. Lett. A*, vol. 319, No. 1-2, (Dec. 2003), 211-216, ISSN 0375-9601.

Schneider, H. & Liu, H.C. (2007). *QuantumWell Infrared Photodetectors. Physics and Applications*, Springer Berlin Heidelberg New York, ISBN-10 3-540-36323-8.

Schöwalter, M.; Rosenauer, A. & Gerthsen, D. (2006). Influence of surface segregation on the optical properties of semiconductor quantum wells. *Appl. Phys. Lett.*, vol. 88, No. 11, (2006), 111906, ISSN 1077-3118.

Stöhr, A.; Humbach, O.; Zumkley, S.; Wingen, G.; David, G.; Jäger, D.; Bollig, B.; Larkins E. C. & Ralston, J. D. (1993). InGaAs/GaAs multiple-quantum-well modulators and switches. *Opt. Quant. Electronics,* vol. 25, No. 12, (Dec. 1993), S865-S883, ISSN 1572-817X.

Tran Thoai, D. B.; Zimmermann, R.; Grundmann, M. & Bimberg, D. (1990). Image charges in semiconductor quantum wells: Effect on exciton binding energy. *Phys. Rev. B*, vol. 42, No. 9, (1990) 5906-5909, ISSN 1098-0121.

Turner, D.B.; Stone, K.W.; Gundogdu, K. & Nelson, K.A. (2009). Three-dimensional electronic spectroscopy of excitons in GaAs quantum wells. *J. Chem. Phys.,* vo.l. 131, (2009), 144510, ISSN 0021-9606.

Tsu, R. & Esaki, L. (1973). Tunneling in a finit superlattice. *Appl. Phys. Lett.*, vol. 22, No. 11 (1973), 562-564, ISSN 1077-3118.

Unlu, S.; Karabulut, I. & Safak H. (2006). Linear and nonlinear intersubband optical absorption coefficients and refractive index changes in a quantum box with finite confining potential. *Physica E: Low-dimensional Systems and Nanostructures,* vol. 33, No. 2, (2006), 319–324, ISSN 1386-9477.

West, L.C. & Eglash, S.J. (1985). First observation of an extremely large-dipole infrared transition within the conduction band of a GaAs quantum well. *Appl. Phys. Lett.*, vol. 46, No. 12, (1985), 1156-1158, ISSN 1077-3118.

Wu, S.; Huang, Z.; Liu, Y.; Huang, Q.; Guo, W. & Cao, Y. (2009). The effects of indium segregation on exciton binding energy and oscillator strength in GaInAs/GaAs quantum wells. *Superlatt. Microstruct.*, vol. 46, No. 4, (Oct. 2009), 618-626, ISSN 0749-6063.

Xie, W. (2010). Laser radiation effects on optical absorptions and refractive index in a quantum dot. *Opt. Commun.* vol. 283, No. 19 (Oct. 2010), 3703-3706, ISSN 0030-4018.

Yablonskii, A. L.; Dzyubenko, A. B.; Tikhodeev, S. G.; Kulik, L. V. & Kulakovskii, V. D. (1996). Dielectric enhancement of magnetoexcitons in surface quantum wells. *JETP Lett.*, vol. 64, No. 1, (July 1996), 51-56, ISSN 1090-6487.

Yang R. Q. (1995). Optical intersubband transitions in conduction-band quantum wells. *Phys. Rev. B* vol. 33, No. 16, (Oct. 1995-II), 11958-11968, ISSN 1098-0121.

Zhao, H.; Chen, Y.T.; Yum, J. H.; Wang, Y.; Zhou, F.; Xue, F; & Lee, J.C. (2010). Effects of barrier layers on device performance of high mobility $In_{0.7}Ga_{0.3}As$ metal-oxide-semiconductor field-effect-transistors. *Appl. Phys. Lett.* Vol. 96, No. 10, (2010), 102101, ISSN 1077-3118.

Zheng, R.S. & Matsuura, M. (1998). Exciton binding energies in polar quantum wells with finite potential barriers. *Phys. Rev. B*, vol. 58, No. 16, (1998), 10769-10777, ISSN 1098-0121.

Xie, W. (2010). Laser radiation effects on optical absorptions and refractive index in a quantum dot. *Opt. Commun.* vol. 283, No. 19, (Oct. 2010), 3703-3706, ISSN 0030-4018.

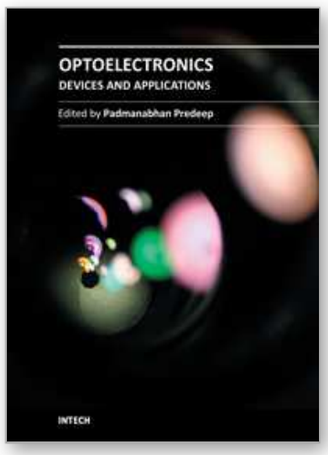

Optoelectronics - Devices and Applications

Edited by Prof. P. Predeep

ISBN 978-953-307-576-1
Hard cover, 630 pages
Publisher InTech
Published online 03, October, 2011
Published in print edition October, 2011

Optoelectronics - Devices and Applications is the second part of an edited anthology on the multifaced areas of optoelectronics by a selected group of authors including promising novices to experts in the field. Photonics and optoelectronics are making an impact multiple times as the semiconductor revolution made on the quality of our life. In telecommunication, entertainment devices, computational techniques, clean energy harvesting, medical instrumentation, materials and device characterization and scores of other areas of R&D the science of optics and electronics get coupled by fine technology advances to make incredibly large strides. The technology of light has advanced to a stage where disciplines sans boundaries are finding it indispensable. New design concepts are fast emerging and being tested and applications developed in an unimaginable pace and speed. The wide spectrum of topics related to optoelectronics and photonics presented here is sure to make this collection of essays extremely useful to students and other stake holders in the field such as researchers and device designers.

INTECH
open science | open minds

InTech Europe
University Campus STeP Ri
Slavka Krautzeka 83/A
51000 Rijeka, Croatia
Phone: +385 (51) 770 447
Fax: +385 (51) 686 166
www.intechopen.com

InTech China
Unit 405, Office Block, Hotel Equatorial Shanghai
No.65, Yan An Road (West), Shanghai, 200040, China
中国上海市延安西路65号上海国际贵都大饭店办公楼405单元
Phone: +86-21-62489820
Fax: +86-21-62489821

IntechOpen